Construction and Building Materials 235 (2020) 117502

Contents lists available at ScienceDirect

Construction and Building Materials

journal homepage: www.elsevier.com/locate/conbuildmat

Elevated temperature, freezing-thawing and wetting-drying effects on polypropylene fiber reinforced metakaolin based geopolymer composites

Yurdakul Aygörmez [a,*], Orhan Canpolat [a], Mukhallad M. Al-mashhadani [b], Mucteba Uysal [c]

[a] Yildiz Technical University, Civil Engineering Department, Davutpasa Campus, Istanbul, Turkey
[b] Istanbul Gelisim University, Civil Engineering Department, Avcilar Campus, Istanbul, Turkey
[c] Istanbul University-Cerrahpasa, Civil Engineering Department, Avcilar Campus, Istanbul, Turkey

HIGHLIGHTS

- Polypropylene fiber reinforced metakaolin geopolymer composites were fabricated.
- Metakaolin was partially replaced with silica fume and colemanite waste.
- Effects of Elevated tepmeratures, freeze-thaw and wetting drying cycles were examined.
- Up to certain extents, the used materials enhanced different porperties of the matrix.

ARTICLE INFO

Article history:
Received 25 September 2019
Received in revised form 1 November 2019
Accepted 5 November 2019
Available online 13 November 2019

Keywords:
Geopolymer
Metakaolin
Silica fume
Colemanite waste
High temperature
Freezing-thawing
Wetting-drying
Polypropylene fiber
Air entraining admixture

ABSTRACT

In this study, metakaolin-based geopolymer samples produced by substitution of silica fume and colemanite waste up to 20% were subjected to high-temperature effects at 300, 600, 900 °C, the wetting-drying effect of 5, 15 and 25 cycles and freezing-thawing effect of 56 and 300 cycles. At the end of the tests, compressive and flexural strengths, ultrasonic pulse velocity and weight changes' results were examined. In addition to these, micro-computed tomography (CT), XRD and SEM analyses were performed to examine the microstructure properties as well as visual inspection. 5 series produced for high temperature and wetting-drying effects were also produced with polypropylene fiber. It has been observed that samples exposed to 900 °C maintained their stability. Polypropylene fiber has been shown to increase the samples' flexural strength results compared to the non-fiber samples after exposing to high temperatures. For the freezing-thawing effect, air-entraining admixture was added to 5 series. An increase for compressive strength was seen after 56 cycles but a decrease was seen after 300 cycles. The geopolymer samples thus began to suffer the real distortion effect in subsequent cycles after the freezing-thawing effect, which contributed to geopolimerization in a sense occurring in the first 56 cycles. During the wetting-drying cycles, fluctuations were observed in the results and an increase in the compressive strength, UPV and weight changes' results after 5 cycles, a decrease in the results after 15 cycles and an increase again in the results after 25 cycles were seen.

1. Introduction

The production of ordinary Portland cement (OPC) is known as an important parameter that triggers emissions by taking second place in the production of greenhouse gasses. Emissions from cement production are expected to increase further in the upcoming years, and it is clear that global warming indices are also affected. In this context, the evaluation of by-products from different industries as admixtures in concrete as well as in cement provides improved properties and plays a role in reducing environmental impacts [1–2]. Geopolymer is an inorganic polymeric material which is prepared by activating the aluminosilicate materials such as fly ash or metakaolin with activators, which becomes reaction products by polycondensation and fragmentary dissolution in alkaline conditions. Due to the high strength and small energy consumption, geopolymers are an alternative to OPC products and eco-friendly [3–4]. Previous studies have shown that geopolymers are superior in terms of strength properties,

* Corresponding author.
E-mail address: aygormez@yildiz.edu.tr (Y. Aygörmez).

https://doi.org/10.1016/j.conbuildmat.2019.117502
0950-0618/

chemical effects, high temperature, and impact resistance compared to Ordinary Portland Cement samples [5,6].

Based on these facts, the properties of the fabricated matrix led the research community to incorporate the field with the recent research technologies and experimental investigations such as rheology tests and 3D printing technologies, [7–9] examined the feasibility of manufacturing geopolymeric matrix using 3D printing technology and conducted various experiments on the resulted specimens. They concluded that more sustainable outcomes could be manufactured with the resulting materials.

On the other hand, when the difference for chemical structure's thermal evolution is examined, it is seen that geopolymer has higher fire resistance than OPC [3,10–12]. Zuda et al. [13] investigated using lightweight composite material with the binding material activated by the activator. A fire protective layer application was made for Portland cement-based buildings. For this reason, a mixture of expanded vermiculite and electric porcelain was used to make aggregate resistant to heating. Up to 1200 °C, mechanical, physical, thermal, water vapor transport and water properties were investigated. Even at 1200 °C, the compressive strength showed 30% and flexural strength showed 3.5 times more performance than the control sample.

In general, for OPC, under the influence of fever, the rate of temperature rise decreases after reaching an estimated temperature of 800 °C in the first 30 min and reaches a constant temperature between 1000 and 1100 °C within nearly 2.0–2.5 h [14]. If concrete is constantly exposed to such extreme fire, serious damage and shedding will occur. Damages change the balance of the reinforcement and consequently cause the collapse of the structure, which increases economic costs and poses a significant risk to human life. Portland cement pastes are the main reason for the formation of this condition, while mechanical properties are weakened by the decomposition of hydration products. In alkali-activated concrete, partial sintering is observed with high temperature and it is thought that compressive strength will increase for this reason [15–17]. Davidovits has demonstrated that fire resistance for 1200 °C is achieved with an activator containing sodium and potassium [18]. Barbosa and MacKenzie found nearly the same results for mixtures with sodium hydroxide and sodium silicate [19]. It is seen that water loss between 100 and 200 °C and 250 to 800 °C causes contraction; no dimensional changes were observed in the samples. Above 800 °C, density and volume changes occurred due to new phases' crystallization. It is thought that this contraction isn't because of a melting point or a viscous flowing process. This contraction is thought to end suddenly between 880 and 900 °C. It is seen that the samples retain their structural stability until they melt at temperatures of 1000–1300 °C. Bakharev detected shrinkage cracks and a slight decrease in strength associated with a rapid increase in average pore size and degradation of aluminosilicates for sodium-activated fly ash based samples at 800 °C [16]. Martin et al. compared alkali-activated fly ash based cements with OPC [20]. Samples showed strength increase after 600 °C while OPC samples lost strength [21].

Duan et al. [22] examined the microstructure, weight loss, and residual strength properties by applying thermal cycles to FA-based geopolymer samples with silica-fume additive. Heating-cooling cycles of 7, 28 and 56 were performed at 200, 400 and 800 °C. It was observed that silica-fume additive increased the strength. At the end of the heating–cooling cycles, the strength and weight loss were seen to be proportional to the increasing temperature. Although the rate of decrease in strength was almost the same with the addition of silica fume, the strengths were better with silica fume after the cycles.

Kong and Sanjayan [23] examined the F-class fly ash-based geopolymer pastes and mortars. Samples were exposed to 800 °C in order to see the loss of strength caused by thermal damage. Geopolymer paste samples showed an increase of 53% in strength and geopolymer mortar samples showed a decrease of 65% in strength. The test showed that the aggregates were exposed to 1.5–2.5% expansion after 800 °C temperature, resulting in loss of strength.

Zhang et al. [24] examined the degree to which the bond strength of geopolymers was affected by high or room temperature. 18 different mixtures of metakaolin and fly ash binder materials were tested at temperatures between 20 and 300 °C. SiO_2/K_2O ratio, Si/Al ratio, fly ash content and solid–liquid ratio were taken as test parameters. In addition to these parameters, additives such as short carbon fibers, styrene acrylate emulsion, and basalt fibers were used. It was observed that short carbon fibers did not affect the degree of bonding at room temperature but limited the cracks at 100–300 °C. Similarly, epoxy resin was found to increase the degree of bonding in the range of 100–300 °C.

Ranjbar et al. [25] examined the geopolymer mortar produced using palm oil fuel ash and fly ash binder materials in terms of compressive strength and microstructural by exposing to high temperatures in the early stages. It was observed that the micropore formation accelerated in the samples after high temperatures and the peak of strength was shifted from 300 to 500 °C.

Türker et al. [26] compared the Ordinary Portland Cement with alkali-activated mortars produced using slag mortars to a high temperature of 800 °C. Test results showed significant differences between slag and Portland cement mortars in the high-temperature resistance. After exposing to 800 °C, the reduction in flexural strength and compressive strength was about 80%.

Two effective raw materials used for alkali activation are fly ash and metakaolin. Preferred reasons include both SiO_2 and Al_2O_3 as the amorphous source in a single material. Borges et al. investigated the engineering properties of alkali-activated metakaolin and metakaolin/slag based mortars. 100% MK-based geopolymer mortars were compared by using dissimilar SiO_2/Na_2O molar ratios with 40% slag added samples. The results indicated that with the slag, the capillary absorption and porosity decreased and the microstructure changed considerably. In addition, with the addition of slag, it has been observed that the required activator ratio for sufficient workability decreased and the strength increased [27].

Metakaolin has high pozzolanic properties and it is produced using high temperatures (500–900 °C) for calcining kaolin [23]. Metakaolin which forms a strong matrix with them when different activators are used provides particularly high strength [28–30]. Davidovits has achieved very high mechanical and durability results by using metakaolin and slag as a source in geopolymer composite production [18]. The type of metakaolin, concentration, and quantity of activator solution and curing conditions become important while the metakaolin used plays a role in the geopolymerization reaction. There are many studies on the production of different types of geopolymers using metakaolin [31–35].

In addition to using fly ash and metakaolin as the essential binder materials in the production of geopolymers, it is also possible to treat different waste materials as binder materials. Turkey has the largest boron deposits and nearly 72% of the available boron in the world. Boron mine can be used in different fields such as energy, agriculture, and medicine. An estimated 1.72 million tonnes of boron compounds and minerals are known to be fabricated in Turkey [36]. Tincal, ulexite, and colemanite are important products. Colemanite is called calcium borate mineral with a hardness of 4 to 4.5 and its specific gravity is 2.4 g/cm^3. The B_2O_3's content in pure colemanite is 51% and after concentration the perborates, sodium borates and boric acid are formed. In addition, a large number of by-products are produced. The effects of these by-products affect the environment in a negative way. The colemanite wastes

pollute the existing underwater resources and have brought negative results. One of the most suitable methods to reduce the negative effects of colemanite is to be considered as a mineral additive in the concrete and cement sector [36,37]. Kula et al. studied the engineering properties of the samples produced using colemanite together with bottom and fly ash. B_2O_3 content becomes important here [38]. It has been determined that the mortar produced by using 10% colemanite wastes as additives increases the mechanical properties [39].

In addition, silica fume can be widely used to improve cement and concrete microstructure [40–42], strength [43–44], durability [45–47]. However, investigations on silica fume added geopolymer composites have failed to satisfy. Chindaprasirt et al. studied the durability properties of FA-based geopolymer and used silica fume for increasing strength and resistance under the influence of acid and sulfate. 3.75% silica fume added geopolymer had an optimum compressive strength (17.0 MPa) in 28 days. The residual compressive strength results of the 5.75% silica fume added geopolymer sample was higher than the control samples under the influence of 5% magnesium sulfate and 3% sulfuric acid solutions [48]. Rostami and Behfarnia investigated the permeability and strength of alkali-activated slag concrete by replacing slag with silica fume. The results showed that by replacing the silica fume, its permeability can be reduced and its compressive strength can be improved, and water curing is the most appropriate method [49].

Fibers with different geometric properties and materials used in the structural application are divided into two categories: low modulus (non-metallic) and high modulus (metallic) [50]. The fiber in each category improves the specific properties of the matrix. In general, metallic fibers provide increased bending strength due to their high stiffness, while non-metallic fibers manage matrices' plastic shrinkage as they have a higher surface contact area and aspect ratio [51]. Polypropylene and steel fibers are widely used in fiber reinforced concrete applications [52]. An increase in impact resistance is achieved with polypropylene fibers to improve the performance of concrete; strain is increased against failure; a thin cracked free surface; it is more resistant to water permeability and consequently improved durability [53]. However, the use of the fibers is limited, as the workability is reduced by adding the fibers to the cemented matrices at a high rate; using the fibers optimally, the interaction between the surface and the matrix can be increased so that it is considered an effective solution to increase the engineering properties of the composites [54–55]. Sukontasukkul et al. examined the strength performance of the geopolymer composites with polypropylene and steel fibers. As a general result, by hybridization of steel fiber can increase toughness, residual strength of the reinforced geopolymer composites with polypropylene fiber. It has been found that both the second peak and the load drop are improved. With the increase of steel fiber, strength and residual strength have gradually improved [56].

Bhutta et al. [57] conducted research on the appropriate fiber reinforcement for strengthening the matrix properties of geopolymer composites. Polypropylene and macro-steel reinforced geopolymer composites were found to be better at flexural strength. Three different types of straight, length-deformed, end-deformed steel fibers and length-deformed polypropylene fiber were used. The optimum ratio for fiber was taken into account at 0.5%. The most ductile flexural was observed in the end-deformed steel fiber between three different steel fibers. Polypropylene fibers didn't have any significant effect on compressive strength.

Mohseni [58] investigated the flexural and compressive strength, displacement, water absorption, Si/Al ratio and electrical resistivity properties of MK-based geopolymer concrete containing polypropylene fibers with 0.3, 0.5 and 1% ratios. The results showed that flexural strength increased by 28% using polypropylene fiber. In addition, if the sodium silicate/sodium hydroxide ratio was considered as 3 and the polypropylene was used as 1%, it showed that the most ideal mixture was obtained in terms of structural, environmental and economic terms.

An important technological breakthrough in the construction industry in the last century is air-entraining agents (AEA). AEA benefits by producing air voids in addition to gel and capillary pores [59]. AEA is often added to fresh cement mixtures to improve processability and consistency, reduce decomposition and bleeding, and increase durability [59–61]. Another benefit of the AEA is that it reduces thermal conductivity by increasing the air content that provides resistance to heat flow [62,63]. The present disadvantage of air entrainment is that it decreases compressive strength by increasing porosity and subsequent reduction of total density. In contrast, the reduction in strength can be compensated by the AEA due to its water-reducing effect. In addition, it has been confirmed in other studies that an increase in air bubbles with this additive has a significant effect on frost resistance [64].

Studies on the freezing-thawing resistance of geopolymers are limited and studies have often investigated the freezing-thawing effect of the external environment. Vegas et al. investigated the freezing resistance of blended cement comprising calcined paper sediment and conducted freezing-thawing tests for dissimilar waste paper sediment calcined containings [65]. Chul-Woo et al. focused on investigating the strength of concretes containing silica fume and fly ash exposed to combined degradation mode [66]. Yawei et al. researched alkali-activated slag concrete's damage mechanics models under the influence of freezing-thawing cycle test [67]. Susan et al. examined the engineering properties of alkali-activated metakaolin/slag concrete [68]. Peijiang et al. examined the resistance of FA-based mortars exposed to freezing-thawing test with curing in ambient conditions and discussed the composition tailoring's importance [69].

Cai et al. [70] examined alkali-activated slag concrete with freezing-thawing resistance. The samples showed excellent resistance at the end of the test and the coefficient of resistance for freezing-thawing was found to be approximately 90%. Yunsheng et al. [71] made freezing-thawing and sulfuric acid tests on fly ash geopolymer composites produced using polyvinyl alcohol fiber. After 20 freezing-thawing cycles test and 1 month exposure to sulphuric acid solution, the samples showed no effect on stiffness and impact strength.

Wetting-drying cycle tests are applied to measure the resistance against the effects of sudden weather conditions. These conditions, together with the deterioration of the building materials, drying shrinkage in consequence of water evaporation in hot weather, and the formation of cracks due to sudden climate change, results in reduced strength or material collapse [72].

The main objective of this study is to examine the high-temperature effect on the geopolymer composites produced using metakaolin partially replaced with silica fume and colemanite waste and its behavior under the effects of freezing-thawing and wetting-drying cycles. On the other hand, there are limited studies on the geopolymer composites' behavior with the polypropylene fiber under the high temperature and wetting-drying effects and with the air-entraining agent under the effect of freezing-thawing. Thus, polypropylene fiber-reinforced and none-fibrous series of geopolymer samples were exposed to 300, 600, 900 °C. In the same way, the series with and without air-entraining admixture was subjected to the freezing-thawing effect of 56 and 300 cycles. Also, the durability tests included the wetting-drying for 5, 15 and 25 cycles. Compressive and flexural strengths, ultrasonic pulse velocity and weight changes' results were examined. In addition to these tests, micro-computed tomography (CT), XRD and SEM analyses were performed to examine the microstructural properties as well as visual inspection.

2. Experimental

In this study, silica fume and colemanite were used as substitution materials while metakaolin was used as the main binding material. Metakaolin is a fine-grained binder material and it has a high pozzolanic activity with a total $SiO_2 + Al_2O_3 + Fe_2O_3$ ratio of 97.18%. The amount of metakaolin passing through a 45 μm sieve is 0.30%, indicating fine grains. In addition, it has a high reactivity due to its fine-grained properties, because it has a small particle size and a high surface area and therefore having fine grains increases the degree of reaction. The slag was used in 13% of the mixture. The chemical properties of the materials used in this study are given in detail in Table 1. Colemanite, silica fume, metakaolin, and slag were expressed in C, SF, MK and S abbreviations, respectively.

In geopolymer composite mortar samples, the fine aggregate (unit weight is 1.352 kg/m^3 and specific gravity is 2.563 g/cm^3) has been used according to BS EN 196-1. The standard fine aggregate's granulometry, sieve analysis, the limit values are given in Table 2.

In preparation of mortar samples, a mixture of sodium hydroxide (12 M) and sodium silicate as SiO_2/Na_2O = 3.29 M ratio was added as an activator. The properties of sodium hydroxide and silicate are given in Table 3 and Table 4, respectively.

In this study, polypropylene fiber was used to investigate the flexural strength of geopolymer mortars after high-temperature test. Properties of polypropylene fiber are given in Table 5. In addition, air-entraining additive was used in this study. Air entraining additive facilitates the development of a constant air voids system in concrete by increasing the durability of the concrete. The AEA's properties are given in Table 6. Air entraining admixture and polypropylene were expressed in AEA and PP abbreviations, respectively.

Colemanite, silica fume, slag, metakaolin, fine aggregate, sodium silicate, and hydroxide were used to prepare the mixture. The mortar mixes were prepared with binder material/fine aggregate ratio as 1/2.5, sodium hydroxide/binder material ratio as 1/3 and sodium silicate/binder material ratio as 2/3. Previous studies were used for the mixture [73–79]. Table 7 shows the amounts of the materials.

For the geopolymer mortar mixture, 450 g of metakaolin was mixed by using the mixer drill with the activator consisting of Na_2SiO_3 solution and a pre-prepared NaOH solution (12 M) one day before. The activator/binder ratio for this mixture was taken as 1:1. Following this stage, 60 g of slag (13% of the binding material) was added to the mix for increasing the calcium ratio. Fine aggregate was used as aggregate and fine aggregate/binder ratio was taken as 2.5/1. In the final stage, a total of 0.8% by volume polypropylene fiber was added to these 5 series for the high temperature and wetting-drying tests, while a 0.1% by weight air-entraining admixture was added for the freezing-thawing test. The obtained mortar was applied to the molds and then vibrated.

Dissimilar temperatures and times were applied in the previous study as curing conditions. Three different temperatures (40, 60, 80) °C and times (2, 24, 72 h) were applied. In addition, the effect of using a non-flammable oven bag during curing was investigated. The prepared samples were able to be removed from the mold after 2 h as slag was used. After 24 h in room conditions, the samples were cured in the drying oven based upon the previous experimental investigations which the authors have done [80].

Geopolymer samples placed in the molds were removed to be kept at room temperature for 2 h after the vibration was applied and a natural cure was applied for 24 h. Geopolymer specimens were held in the drying oven for 72 h at 60 °C with the non-flammable oven bags following the 24-hour period. The non-flammable oven bags helped for preventing evaporation of water. After heat curing, samples were kept in closed plastic boxes for up to 28 days. After 28 days, high temperature and freezing-thawing, wetting-drying tests were performed.

Table 2
Fine aggregate's gradation and standard limit values.

Characteristic	Grain size (mm)					
	0.08	0.16	0.5	1.0	1.6	2.0
Remaining (%)	99	87	72	34	6	0
Limit (%)	99 ± 1	87 ± 5	67 ± 5	33 ± 5	7 ± 5	0

Table 3
Sodium hydroxide's chemical properties (%).

NaOH	Na_2CO_3	Cl	SO_4	Al	Fe
99.1	0.3	≤0.01	≤0.01	≤0.002	≤0.002

Table 4
Sodium silicate's chemical properties.

Na_2O (%)	SiO_2 (%)	Density (20 °C) (g/ml)	Fe (%)	Heavy metals (as Pb) (%)
8.2	27.0	1.360	≤0.005	≤0.005

Table 5
The properties of polypropylene fiber.

Length (mm)	Diameter (μm)	Specific Gravity	Nominal Tensile Strength (MPa)	Aspect Ratio
12	0.0075	0.91	750	1600

Table 6
The properties of air entraining admixture.

Specific Gravity (kg/l)	PH value	Alkali content (%)	Chlorine ion content (%)
0.98–1.03	9–11	≤10 (by weight)	<0.1 (by weight)

Table 7
Geopolymer mortar mixing proportions (g).

Metakaolin	Fine aggregate	Slag	NaOH (12 M)	Na_2SiO_3
450	1125	60	150	300

Table 1
The binders' chemical properties.

Chemical analysis, %	SiO_2	Al_2O_3	Fe_2O_3	TiO_2	CaO	MgO	K_2O	Na_2O	B_2O_3	L.O.I.
MK	56.10	40.25	0.85	0.55	0.19	0.16	0.55	0.24	–	1.11
S	40.60	12.83	1.37	0.75	36.08	6.87	0.68	0.79	–	0.03
SF	90.58	1.37	0.15	–	0.35	4.02	2.55	0.58	–	0.40
C	5.00	0.40	0.08	–	26.02	3,00	–	0.50	40.00	25.00

It has been found that using colemanite waste up to 10% has a good performance with the advantages of forming a protective layer and filling the voids, and has shown a significant improvement in microstructure due to the relative permeability and brittle of the geopolymeric matrix [81–82]. Thus, boron waste is suitable to use up to 10% in geopolymer composite samples [38]. In previous studies, it has been found that by using boron minerals with cement-based systems, it provides a protective layer for cement particles and restrains contact among cement particles and water. This effect directly influences the hydration mechanism of cementitious materials [83]. In addition, it has been determined that the mechanical properties of cement-based composites are improved under favour of colemanite waste [84].

Silica fume, because it has very fine grains, plays an important role in the process of converting large voids to small ones. In conclusion, similar to the behavior of cemented matrices, it has been shown that geopolymeric matrices provide improvement by reducing voids rates [85]. However, it has been found that silica fume, if used more, reduces the workability and adversely affects the properties of the mortar. The high specific surfaces of the silica fume particles have a negative effect on workability. Table 8 shows the 28 days strength results of 9 mixtures.

When the pre-mix results were taken into consideration, high temperature, freezing-thawing, and wetting drying tests were performed with 5 series (control samples MK, 10SF, 20SF, 10C and 20C) which have the highest results. In the final stage, a total of 0.8% by volume polypropylene fiber was added to these 5 series for the high temperature and wetting-drying tests, while a 0.1% by weight air-entraining additive was added for the freezing-thawing test for the durability properties.

Table 8
Trial mixes for the current research.

Mixes	Compressive strength at 28 d (MPa)	Flexural strength at 28 d (MPa)
100% MK	60.37	10.43
90% MK + 10% SF	59.74	13.17
80% MK + 20% SF	67.30	13.50
70% MK + 30% SF	46.04	10.76
60% MK + 40% SF	43.80	10.38
90% MK + 10% C	61.59	11.95
80% MK + 20% C	47.85	10.97
70% MK + 30% C	43.41	9.61
60% MK + 40% C	33.16	9.02

After the 28 days, geopolymer mortar sample series were subjected to temperatures of 300, 600 and 900 °C in the high-temperature furnace. The samples were dried for 24 h at 105 °C before the test. The temperature increase rate of 5 °C/min was adjusted in the high temperature oven. The samples were kept at maximum temperature for 1 h after reaching the desired temperature. The samples were then allowed to cool down in the oven to avoid thermal shock. The samples were analyzed after heat treatment and mechanical and physical changes were investigated. Flexural and compressive strengths, ultrasonic pulse velocity and weight changes' results were examined. After the 28 days, the geopolymer series were also subjected to the freezing-thawing test with a total of 56 and 300 cycles. In each cycle, the freezing period was set to 90 min, the thawing period was set to 30 min, and the temperature range of the test was set to 4 °C to −18 °C. Wetting-drying test was performed for 28 days samples. The test involved drying the samples at 65 °C for 24 h and then immersing them in water at room temperature for 24 h. This was considered 1 cycle and samples were subjected to 5, 15 and 25 cycles. The same tests were made for freezing-thawing and wetting-drying. For compressive strength 50 mm cubes were used (ASTM C 109) [86], and for flexural strength (ASTM C 348) [87] prismatic molds were used.

3. Results and discussion

The tests in this investigation were conducted based on three categories, namely elevated temperature, freezing-thawing, and wetting drying cycles. The tests are illustrated in (Fig. 1).

3.1. Elevated temperature

3.1.1. Compressive and flexural strength results

Changes in geopolymer samples that were kept under the effect of 300, 600 and 900 °C were investigated. In addition, polypropylene fibers were added to the blends by 0.8% by volume to achieve their effect. After the high-temperature test, flexural and compressive strengths results were compared with the 28 days' results (Figs. 2, 3). After 600 °C, there was a significant decrease in com-

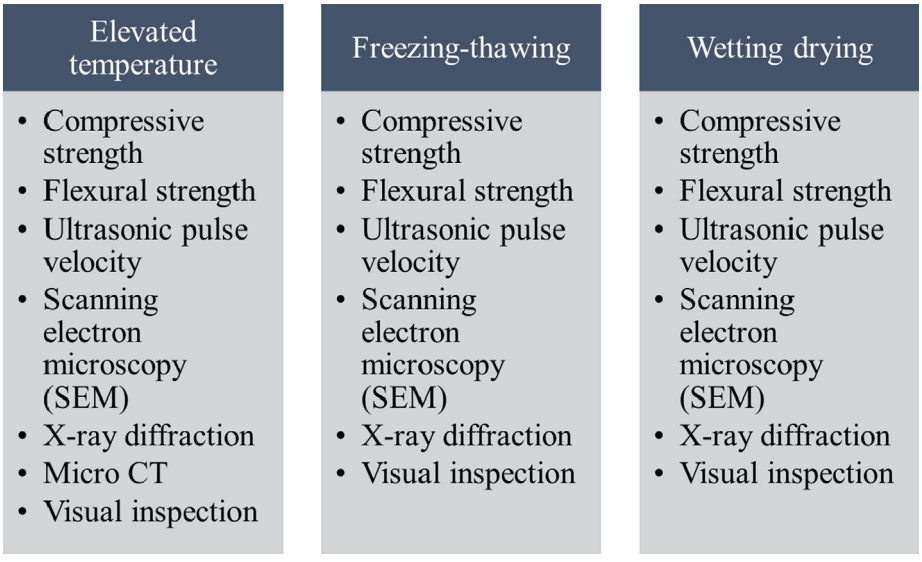

Fig. 1. Classification of the investigation's tests.

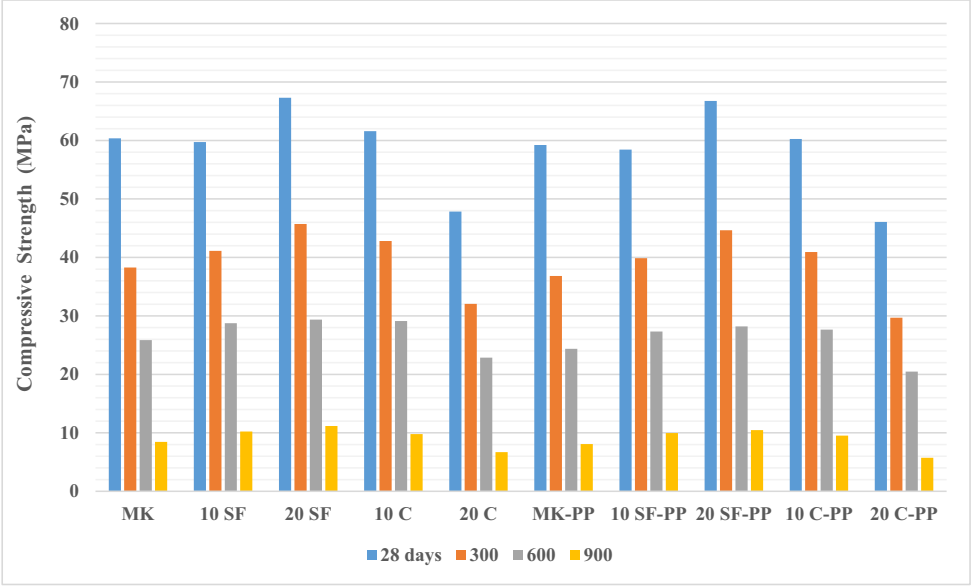

Fig. 2. Residual compressive strength results after high-temperature test.

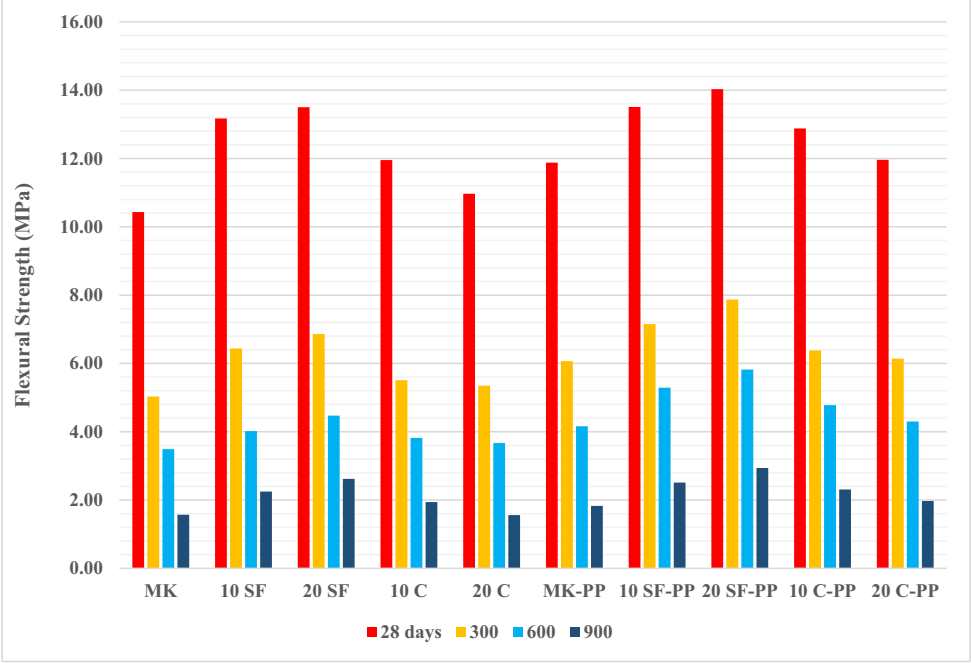

Fig. 3. Residual flexural strength results after high-temperature test.

Table 9
Compressive strength loss rates due to high temperature (%).

	300 °C	600 °C	900 °C
MK	32.61	55.15	86.00
10 SF	31.15	51.89	82.89
20 SF	31.07	50.37	82.40
10 C	31.49	52.70	84.10
20 C	33.02	53.23	86.00
MK-PP	34.82	56.84	86.38
10 SF-PP	32.79	54.26	84.96
20 SF-PP	32.07	53.74	84.32
10 C-PP	32.38	54.10	85.19
20 C-PP	34.55	55.55	86.54

Table 10
Flexural strength loss rates due to high temperature (%).

	300 °C	600 °C	900 °C
MK	54.77	69.54	84.95
10 SF	51.11	67.48	82.92
20 SF	49.19	66.89	80.59
10 C	53.90	68.04	83.77
20 C	54.23	68.54	84.78
MK-PP	48.91	64.98	84.60
10 SF-PP	45.08	60.84	81.42
20 SF-PP	43.91	58.52	79.04
10 C-PP	46.43	62.89	82.07
20 C-PP	47.66	64.05	83.53

pressive and flexural strengths (Tables 9–10). The geopolymer composites' strengths were significantly reduced by a temperature range of 600 °C to 900 °C due to the evaporation of water and dehydration of the geopolymer matrix, the melting of the fibers due to high temperature and the thermal reaction mechanism of free water evaporation [88]. For the geopolymer mortar sample, the decrease for flexural strength with high-temperature effect was higher than compressive strength. This was due to the fact that the flexural strength was more sensitive to the development of internal microstructure defects, such as the propagation of cracks and the growth of porous structures at high temperatures [89].

The compressive strength losses for fiberless geopolymer samples ranged from 31.07% to 86%, whereas this rate increased slightly and ranged between 32.07% and 86.54% in the polypropylene fibrous geopolymer samples. Flexural strength losses for fiberless geopolymer samples ranged from 49.19% to 84.95%, while this rate decreased and ranged between (43.91–84.60) percent in the polypropylene fibrous samples. The goal of adding fiber to cement or geopolymer mortar is to increase flexural strength and improve flexural toughness [90]. Polymer fibers are a widely used type of material for reinforcing geopolymer composites and it has been confirmed that fibers can improve the geopolymer's flexural strength and toughness very effectively [91–95]. Zhang et al. produced polypropylene fiber reinforced calcined kaolin and fly ash based geopolymer composites and it was found that the fibers increased the flexural strength by 38.6% [91]. Al-mashhadani et al. studied the engineering properties of fly ash-based geopolymer composites using steel and polyvinyl alcohol fibers, and it was found that flexural strength increased 39.84% and 31.45% compared to the control sample when using polyvinyl alcohol and steel fibers, respectively [95]. Although it has been claimed that fibers can increase compressive strength [92–93] if used at the appropriate dosage, it is reported a decrease in compressive strength with fiber addition [91,94–95]. There are many harmful pores in fiber-reinforced materials, which can weaken the bond between the fibers and the cement or geopolymer matrix and thus adversely affect the matrix [96–98]. With respect to polypropylene fibers, the decrease in compressive strength is caused by both the low density of the fibers used and the flocculation of the fibers resulting in a decrease in unit weight and compressive strength and an increase in water absorption rate. According to this; it was observed that compressive strength values decreased with polypropylene fiber additive in all blends. Reducing the workability of mortars with increasing fiber addition is known from the studies [99]. In addition to the low modulus that causes low residual stress, polypropylene fibers have been found to be hydrophobic, meaning that they desire to move away from water-based systems [100–101]. Polypropylene fibers also appear to increase porosity while reducing processability; this adversely affects mortar compaction. Polypropylene fiber is more effective in stopping the micro-cracks caused by tensile stresses in the lower regions of the mortar during the flexural strength test, and as a result, the flexural strength increases with increasing fiber yield [102].

Pliya et al. [103] conducted research on the behavior of high strength concrete under high temperatures (150, 300, 450 and 600 °C) using polypropylene and steel fibers. The amount of polypropylene fibers with a length of 6 mm was taken as 1 and 2 kg/m^3. Four heating–cooling cycles were applied to the concrete samples. According to the results of this research, while the

Table 11
Ultrasonic pulse velocity loss rates due to high temperature (%).

	300 °C	600 °C	900 °C
MK	51.25	72.73	77.55
10 SF	48.15	69.09	74.25
20 SF	47.23	68.13	73.82
10 C	48.60	71.45	76.39
20 C	51.22	72.62	76.62
MK-PP	52.68	72.85	78.14
10 SF-PP	50.89	69.64	74.60
20 SF-PP	49.96	68.70	74.28
10 C-PP	50.88	71.11	76.98
20 C-PP	52.03	71.98	77.36

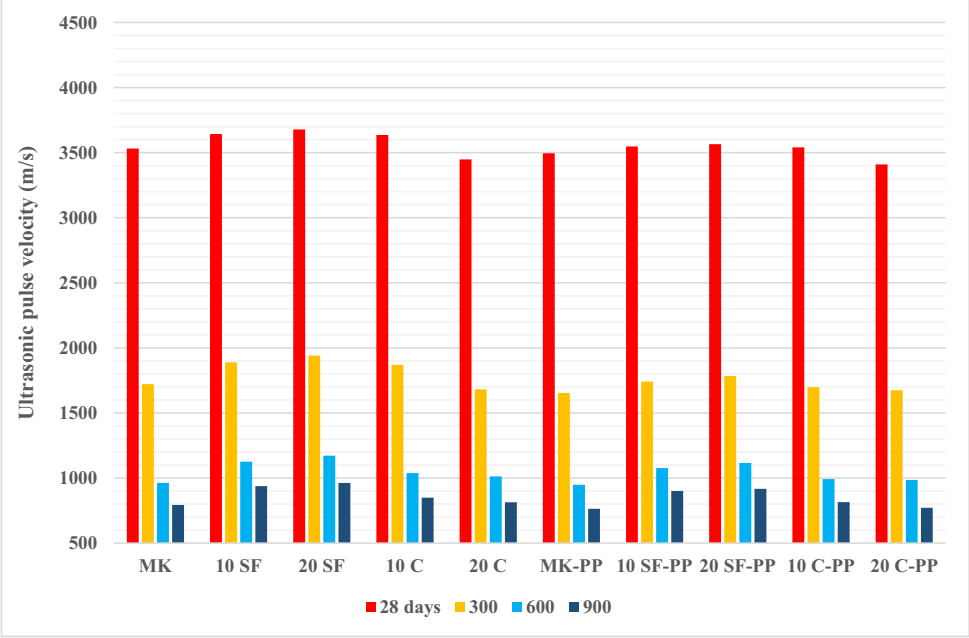

Fig. 4. Ultrasonic pulse velocity results after high temperature test.

polypropylene fibers did not have a significant effect on the remaining compressive strength after reaching 600 °C, samples containing 1 kg/m^3 polypropylene fiber showed higher residual compressive and splitting tensile strength results when heated to 300 °C. Ding et al. [104] used a 15 mm long polypropylene fiber to examine the ultimate load, residual compressive strength, flexural toughness, fracture mode and energy of self-compacting high-performance concrete held at 300, 600 and 900 °C for 3 h. The results indicated that PP fibers had a significant effect on the reduction of surface cracks but did not show a clear effect on the mechanical properties of the concrete. Yermak et al. [105] investigated the behavior of steel and polypropylene fiber reinforced concrete at high temperature. Polypropylene fibers have been found to prevent macroscopic damage of steel fiber concretes during firing. Rudnik and Drzymała [106] focused on the thermal behavior of polypropylene fiber reinforced concrete at high temperatures. Samples were exposed to 100, 200, 300, 400, 500 and 600 °C. The authors concluded that polypropylene fibers had no significant effect on the thermal stability of concrete samples. When the compressive strength results after high temperature were examined, it was observed that the results showed similar behavior to the samples before high temperature. This situation is consistent with the above-mentioned studies. Polypropylene fibers have no effect on compressive strength.

The flexural strength results of the samples after high temperature showed a tendency to grow in contrast to the compressive strength results. Polypropylene fibers can control the cracks formed while reducing the width and number of cracks. This is the main reason for the increase in flexural strength. The positive behavior of the fibers in flexural strength in concrete can be explained by the fiber's short distance and a very large connection in the matrix. Therefore, after microscopic cracks have formed in the composite tissue, the conversion of these microscopic cracks into the macroscopic cracks can be prevented by means of fibers. The fibers continue to withstand the tension and transfer this tension from one end of the cracks to the other until they leave the matrix [107]. In addition, polypropylene fibers melt at 160–170 °C to release pore pressure by forming a free path for escaping water vapor. Thus, it is assumed that surface cracks are very limited or not. Kalifa [108] suggests that molten polypropylene is absorbed by the matrix and plays a role in the pressure relief with empty fiber beds.

The increase in compressive strength seen in silica fume additive geopolymer composites can be attributed to the have a more dense microstructure resulting from the fact that fine silica fume particles acting as a micro-aggregate filler that is dispersing in geopolymer and can fill the inner space in the geopolymer paste's microstructure. On the other hand, the highly reactive pozzolan silica fume reacts with calcium hydroxide formed from the reaction between the calcium oxide in the main binder material and the alkali from the activator mixture. This reaction results in the formation of C-S-H gel. The presence of silica fume particles results in a compact microstructure and strength increase [109–111]. As a result of the pozzolanic reaction between calcium hydroxide and silica fume, more C-S-H is formed in the matrix, which increases the strength development of geopolymer composites [48]. Obviously, after examining the geopolymer composites under the effect of high temperature, it was found that compressive strength was improved by adding silica fume. While it was observed that the compressive strength of each geopolymer composite after high temperature decreased with thermal effects, the results with silica fume were higher than the control sample. The results of compressive strength loss for silica fume additive geopolymer as a result of thermal cycles are consistent with the findings reported previously [112–114]. If colemanite waste is replaced with primary binder material up to 10%, it is possible to influence the results positively. Silica fume and colemanite waste can act similarly in case of substitution and reduce the voids ratio to form a more compact structure. These conditions decreased the rate of deterioration after the high-temperature test and increased the strength compared to the control sample [81,82].

The replacement of SF increased the residual compressive and flexural strengths. The residual compressive strengths were

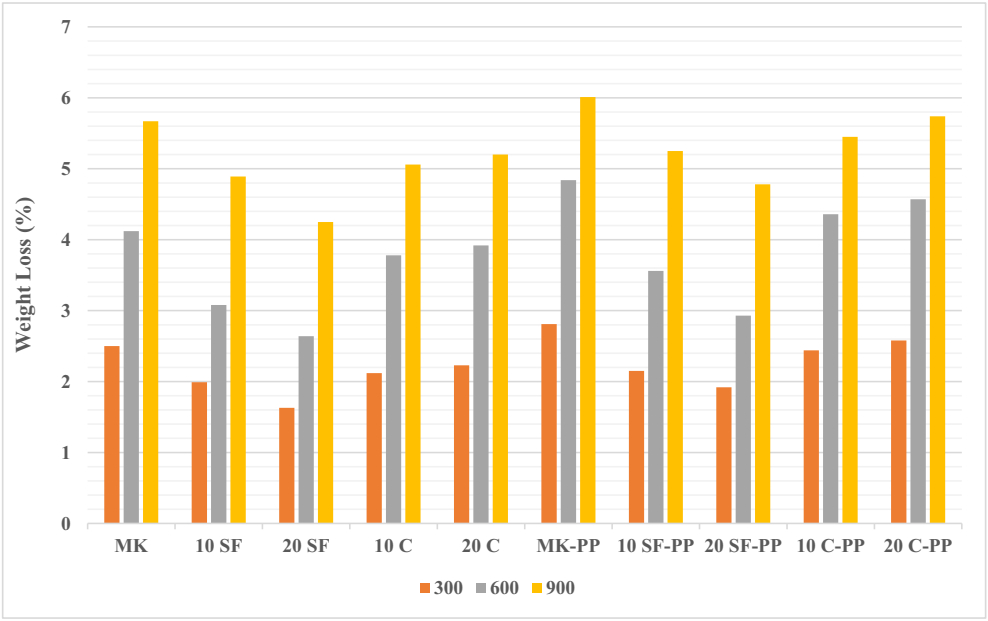

Fig. 5. Weight loss rate results after high temperature test.

45.72 MPa, 29.36 MPa, and 11.17 MPa, respectively, at 300 °C, 600 °C and 900 °C for 20 SF. For 20 SF-PP, at 300 °C, 600 °C, and 900 °C, the residual flexural strengths were obtained as 7.87 MPa, 5.82 MPa and 2.94 MPa, respectively.

Colemanite waste had a positive effect on the replacement of up to 10%. For 10 C samples, the residual compressive strengths were obtained as 42.81 MPa, 29.13 MPa and 9.79 MPa at 300 °C, 600 °C, and 900 °C, respectively. For 10C-PP, the residual flexural strengths

Fig. 6. MK samples exposed to high temperature.

Fig. 7. 10 C samples exposed to high temperature.

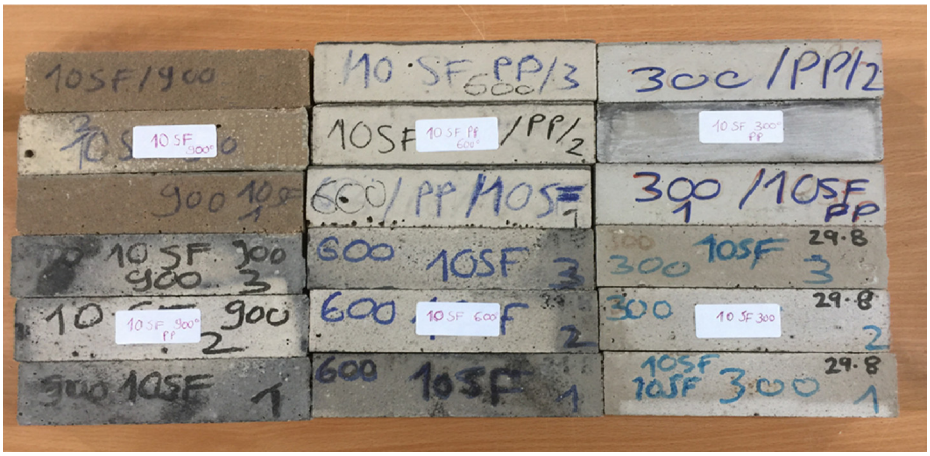

Fig. 8. 10 SF samples exposed to high temperature.

were obtained as 6.38 MPa, 4.78 MPa and 2.31 MPa at 300 °C, 600 °C, and 900 °C, respectively.

3.1.2. Ultrasonic pulse velocity results

As the temperature increases, the sample pore structure's growth and the water evaporation in the matrix increases. Additional voids arise due to the mass loss formed. Additional voids that occur in this way result in lower ultrasonic pulse velocity results [115]. The ultrasonic pulse velocity results and reduced rates of the samples exposed to high temperatures are shown in Fig. 4 and Table 11, respectively. All samples showed similar behavior as a result of high-temperature effects and a significant decrease in UPV values after 300 °C was observed. As a result of the observation, it was determined that serious damages occurred in the solid geopolymeric matrix after the effect of 300 °C and this situation was consistent with the loss of compressive and flexural strength results. In addition, the formation of microfractures accelerated with higher temperature effects and the density of the composites was reduced and the ultrasonic velocity waves' propagation time was prolonged and lower UPV values were formed. Also lower UPV values were formed due to the melting of fibers in the matrix composites and leaving microscopic channels above 300 °C [116]. The results in the fiber series are also consistent before high temperature. Regardless of the temperature effect, there was no significant difference with the addition of polypropylene fibers, on the contrary, it slightly affected the performance of the samples. This is thought to be related to the properties of fibers and their behavior in the geopolymeric matrix [95,102]. The UPV results loss rate in non-fiber geopolymer mortars ranged between 47.23% and 51.25% at 300 °C, between 68.13% and 72.73% at 600 °C and between 73.82% and 77.55% at 900 °C. In fiber geopolymer mortars, a decrease in the rate of ultrasonic pulse velocity was observed between 49.96% and 52.68% at 300 °C, between 68.70% and 72.85% at 600 °C and between 74.28% and 78.14% at 900 °C.

According to the results of the ultrasonic pulse velocity of the samples shown in Figs. 4, 20% silica fume substitution positively affected the post-temperature results. Because the silica fume has fine grains that are dispersed in the microstructure of the geopolymer matrix and act as micro-aggregate fillers, a dense microstructure has been formed, which shortens the propagation of ultrasonic velocity waves [112–114]. Similarly, the addition of colemanite waste had a positive effect on the results up to 10%. Silica fume and colemanite waste can act similarly in case of

Fig. 9. 20 SF samples exposed to high temperature.

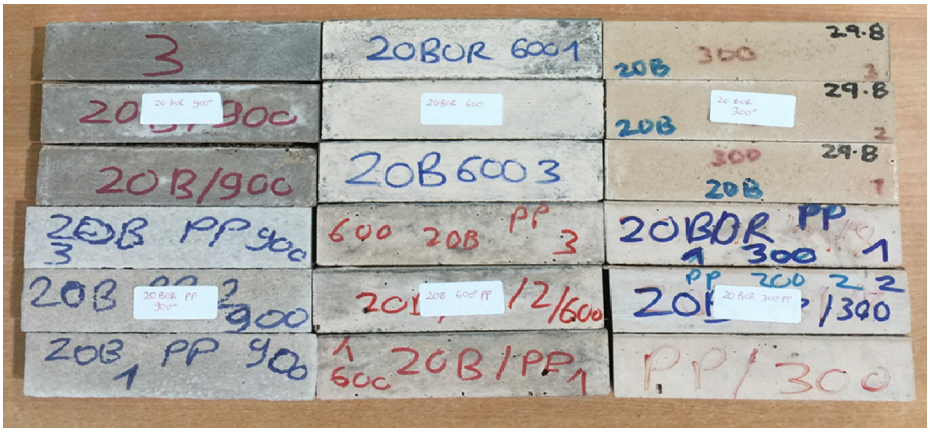

Fig. 10. 20 C samples exposed to high temperature.

substitution and reduce the voids ratio to form a more compact structure. So UPV results were higher with silica fume and colemanite in the geopolymer composites [81]. The residual ultrasonic pulse velocity results in MK samples were 1722 m/s, 963 m/s and 793 m/s at 300 °C, 600 °C and 900 °C, respectively. The residual ultrasonic pulse velocity results in 10C samples were 1869 m/s, 1038 m/s and 850 m/s at 300 °C, 600 °C and 900 °C, respectively. The residual ultrasonic pulse velocity results in 20SF samples were 1941 m/s, 1172 m/s and 963 m/s at 300 °C, 600 °C and 900 °C, respectively.

3.1.3. Weight loss results

The main components of the metakaolin binder material are the amorphous phases Al_2O_3 and SiO_2 and are widely used due to their good mechanical and durability properties as well as a high specific area and less impurity [117]. The geopolymer composites' compressive strength is significantly reduced due to the dehydration of the matrix resulting from the free water evaporation's thermal reaction mechanism and high temperature [88]. The geopolymer's solid matrix suffers serious damage after high-temperature effect and increasing temperatures further increases the expansion of the cracks and increases the loss of compressive strength due to the formation of matrix voids. When the temperature rises, a dehydration reaction occurs and moisture moves towards the sample surface and escapes, this leads to microstructure's internal damage and consequently weight loss in the geopolymer composite [118]. Weight loss in the early stage of heating in the geopolymer sample occurs very quickly due to free water and structured water [119].

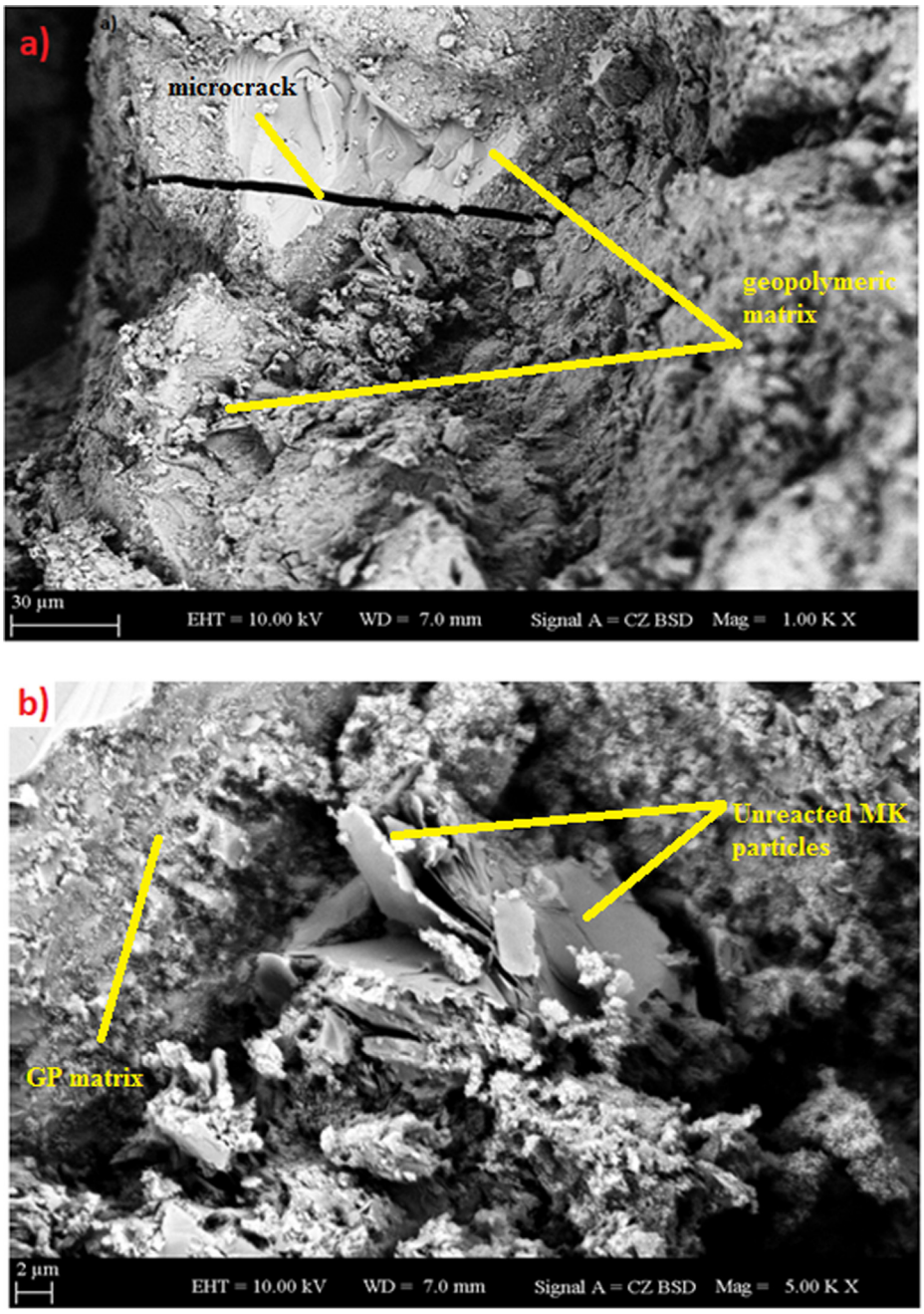

Fig. 11. SEM micrographs of 10 C geopolymer samples after exposure to 300 °C a) magnified 1000 times and b) magnified 5000 times.

Weight loss mainly consists of three forms of water loss: Free, adsorbed and chemically bound water. The weight loss shows a sudden increase above 400 °C. It can be said that most of the resulting weight loss occurs between 400 °C and 800 °C. The main cause of weight loss below 600 °C is the evaporation of condensed hydroxyl groups and free water [120]. Evaporation of water plays a role in this loss, as well as decomposition of unhydrated and hydrated compounds beyond 400 °C. Dehydration begins beyond 400 °C with the release of chemically bound water involved in the formation of internal pores. In addition, viscous sintering in the geopolymeric network shows the main cause of thermal shrinkage due to high temperature effect [121]. The apparent effect increases with increasing temperature, so the shrinking pores of the samples increase the tendency to collapse [82].

It was observed that the increase in weight loss percentage was higher with polypropylene fiber reinforced samples. The main reason for this is that polypropylene fibers above 160 °C melt and create channels in the concrete. This results in more weight loss in fiber samples due to fiber evaporation at high temperatures. At temperatures above 600 °C, these fibers become molten condition and evaporate. At higher temperatures, the polypropylene fiber was completely evaporated. As a result of these parameters' cumulative effects, weight reduction increases in samples with high temperatures [122].

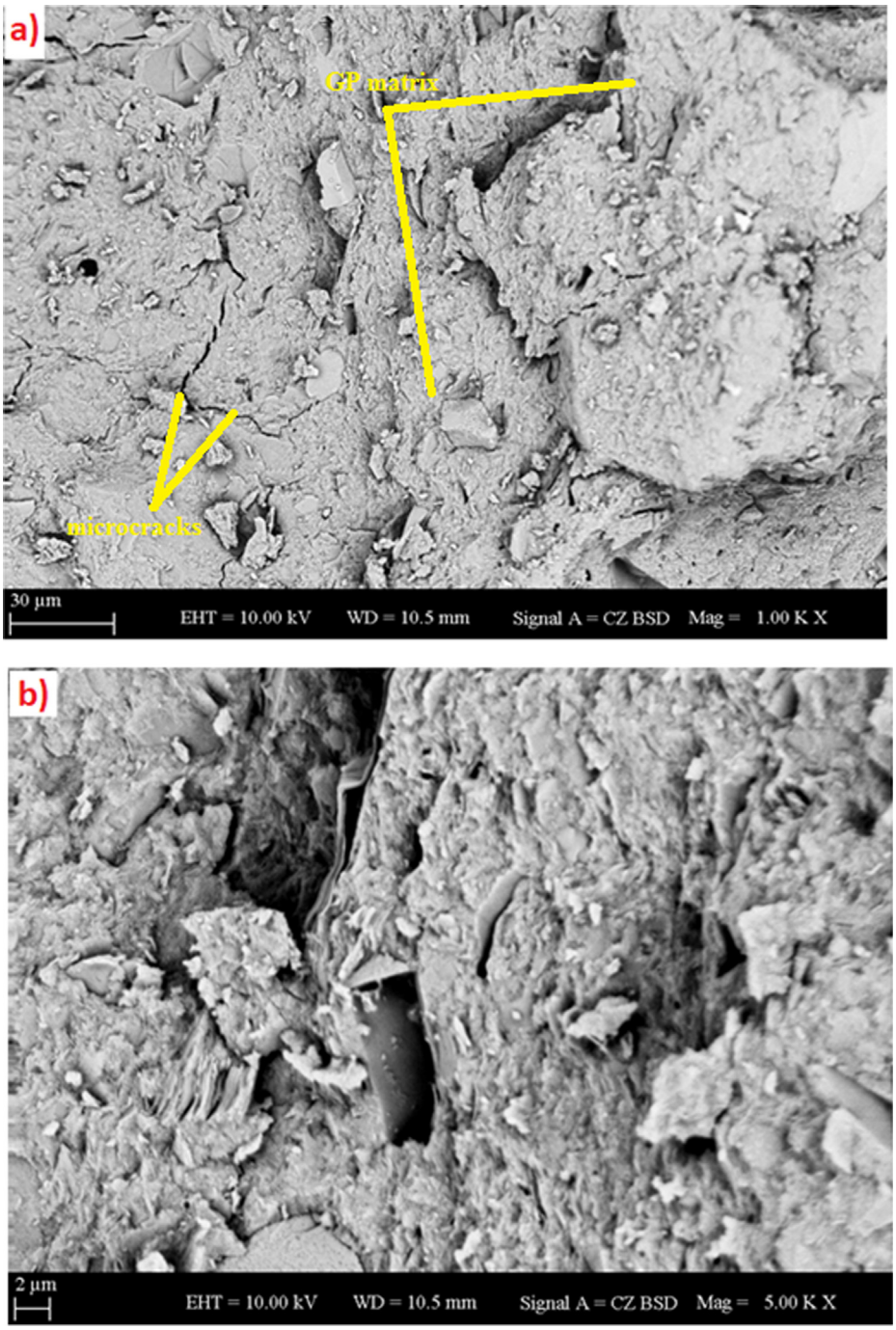

Fig. 12. SEM micrographs of 20 SF geopolymer samples after exposure to 300 °C a) magnified 1000 times and b) magnified 5000 times.

The weight loss results due to high temperature are given in Fig. 5. Weight-loss rates in fiber geopolymer mortars with high-temperature effects were between 1.92% and 2.81% at 300 °C, between 2.93% and 4.84% at 600 °C and between 4.78% and 6.01% at 900 °C. Weight-loss rates in non-fibrous geopolymer mortars were between 1.63% and 2.5% at 300 °C, between 2.64% and 4.12% at 600 °C and between 4.25% and 5.67% at 900 °C. According to the MK sample, silica fume and colemanite waste replacement decreased weight loss. Silica fume and colemanite waste can act similarly in case of substitution and reduce the voids ratio to form a more compact structure. So weight loss results were lower with silica fume and colemanite in the geopolymer composites [81].

3.1.4. Visual inspection of the samples

Changes in the surface of the sample under the high-temperature effect were also examined (Figs. 6–10). The photos were taken immediately after the high-temperature test. When the samples were exposed to 300 °C, there was no significant color change in proportion to the reduction in compressive strength. In the samples exposed to 600 °C, the color change was observed. With a significant loss of compressive strength in the 600 °C–900 °C range, cracks have started to be seen. After 900 °C, geopolymer samples had a significant amount of color change, but the cracks remained at a lower rate. This was consistent with the fact that geopolymer specimens maintained stable conditions under

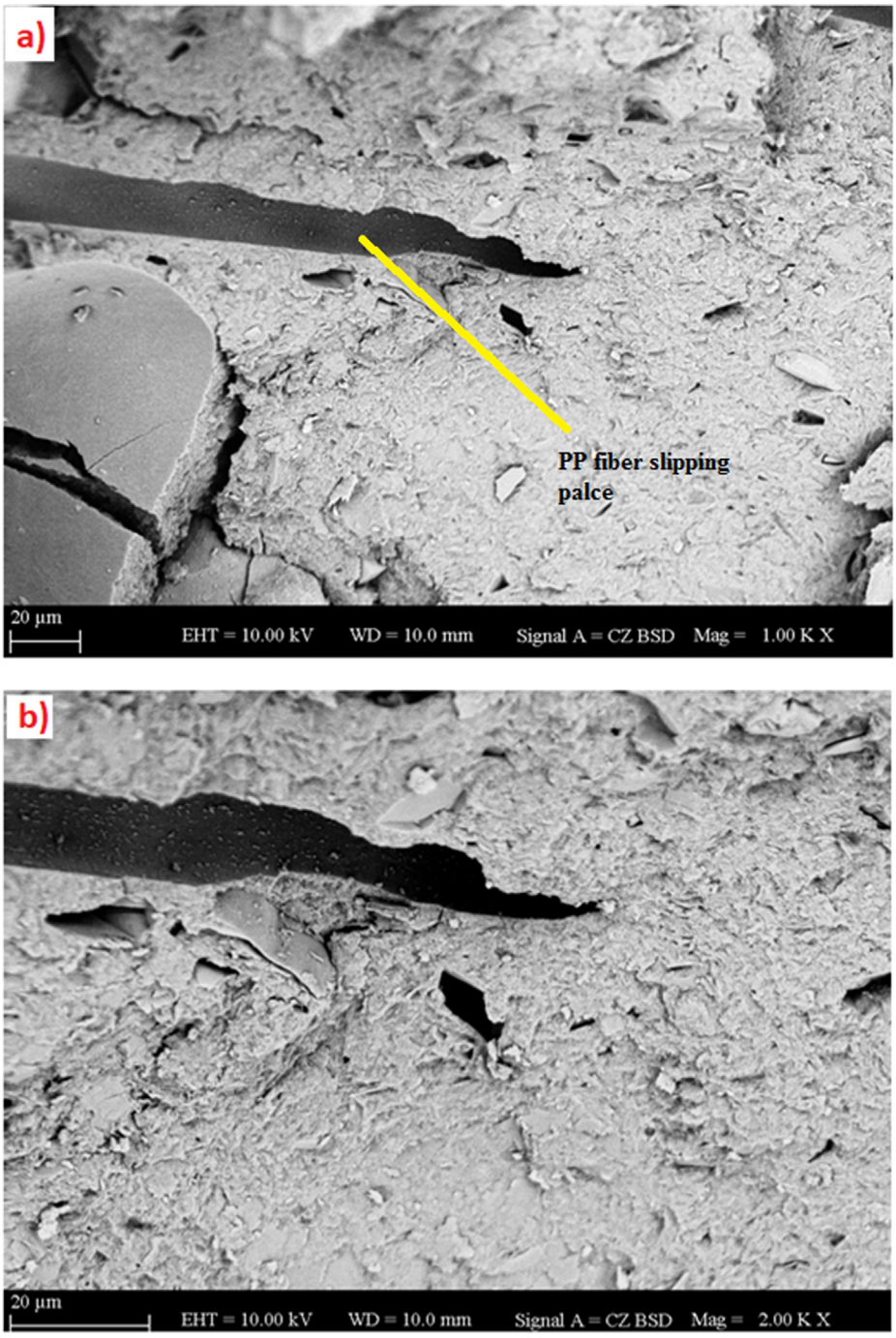

Fig. 13. SEM micrographs of 10C geopolymer samples after exposure to 600 °C a) magnified 1000 times and b) magnified 2000 times.

high-temperature influence. The samples' surface had a tendency to be a little coarser [82,123].

To get an idea about the geopolymeric matrix with its bonding degree, scanning electron microscopy (SEM) was performed for 10 C and 20 SF samples after heat treatment with 300 °C and 600 °C. In addition, when the microstructural analysis is examined, it will be possible to have an idea about the variation of the relations between the microstructure and mechanical properties of geopolymer samples with elevated temperature. Microstructural changes in 10 C and 20 SF samples after exposure to 300 °C and 600 °C are shown in Figs. 11–14. The microstructure of specimens was preserved after exposure to 300 °C. No significant damage to the specimens occurred when exposed to 300 °C. The microstructure of metakaolin-based geopolymer samples became more porous due to weight loss, matrix decomposition, and phase transformations when exposed to high temperatures after 500 °C. Although deformations and macrostructural crack formation are seen in Figs. 13–14, the microstructure remains unchanged after thermal attack; however, a decrease in porosity for samples was observed at 600 °C compared to 300 °C temperature. The formation of silica-rich gels as reaction products in the geopolymeric gel may produce a decrease in pore volume after high temperature, which is believed to result in a high densification level and cause the structure to collapse at about 600–750 °C; moreover, it is

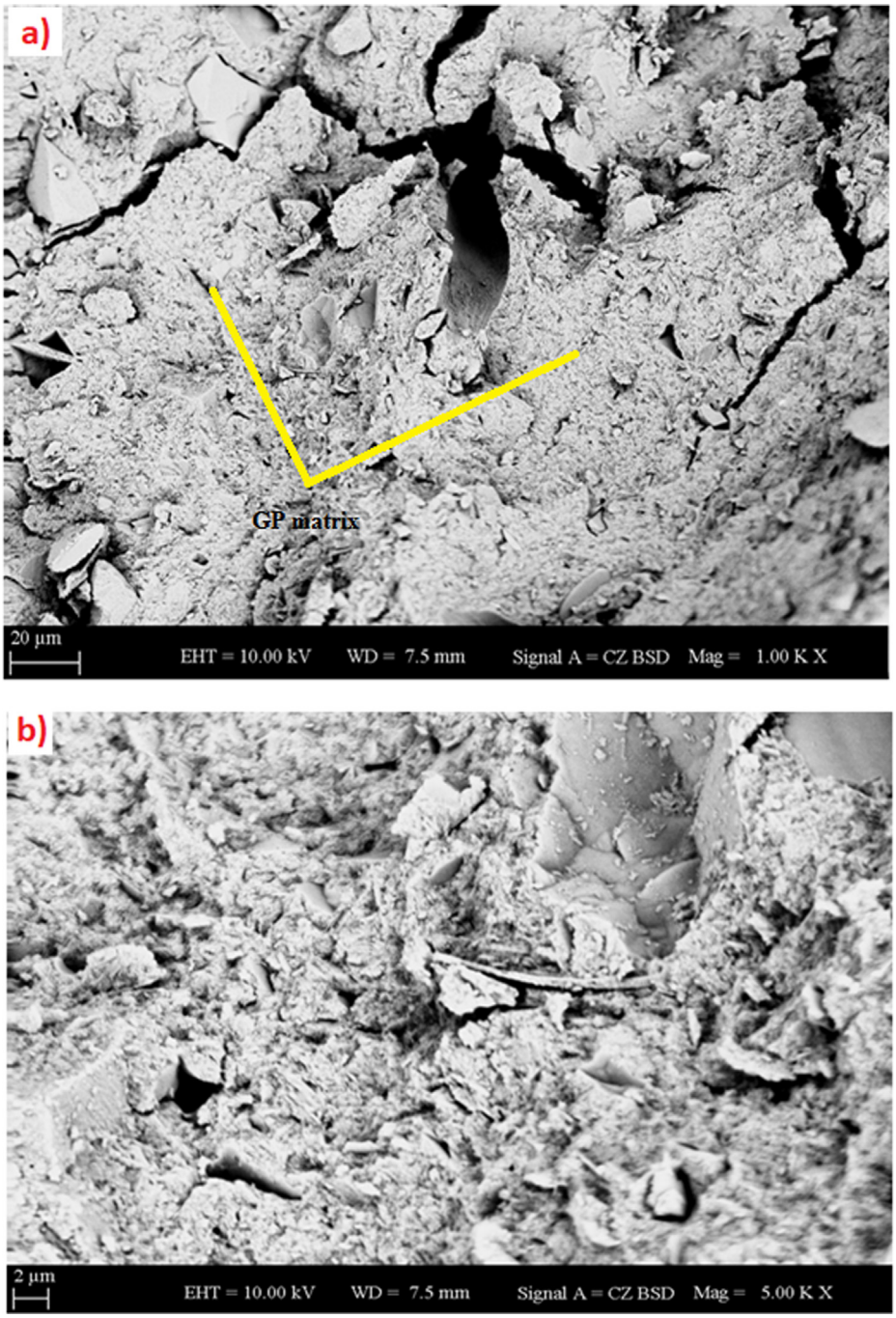

Fig. 14. SEM micrographs of 20 SF geopolymer samples after exposure to 600 °C a) magnified 1000 times and b) magnified 5000 times.

determined that the initial densification temperature decreases with the increment in Si/Al ratio [124]; These factors promoted to the pore reduction for synthesized geopolymers. Acceleration in pore volume reduction and water loss in the geopolymer with evaporation and dehydroxylation after thermal attack can cause the structural defects or the defects formation intensifying; these effects can also contribute to loss of strength after thermal attack. In addition, new crystal phases formed by redistribution of atoms due to uncontrollable diffusion result in loss of strength seen in the samples. In spite of this situation, the basic structure of classical metakaolin-based geopolymers was preserved according to the XRD results, and geopolymer materials showed lower microstructural deterioration at higher temperatures and therefore showed less strength loss [82,125].

XRD technique can be used to better understand possible transformations in mortar samples that have been affected by high

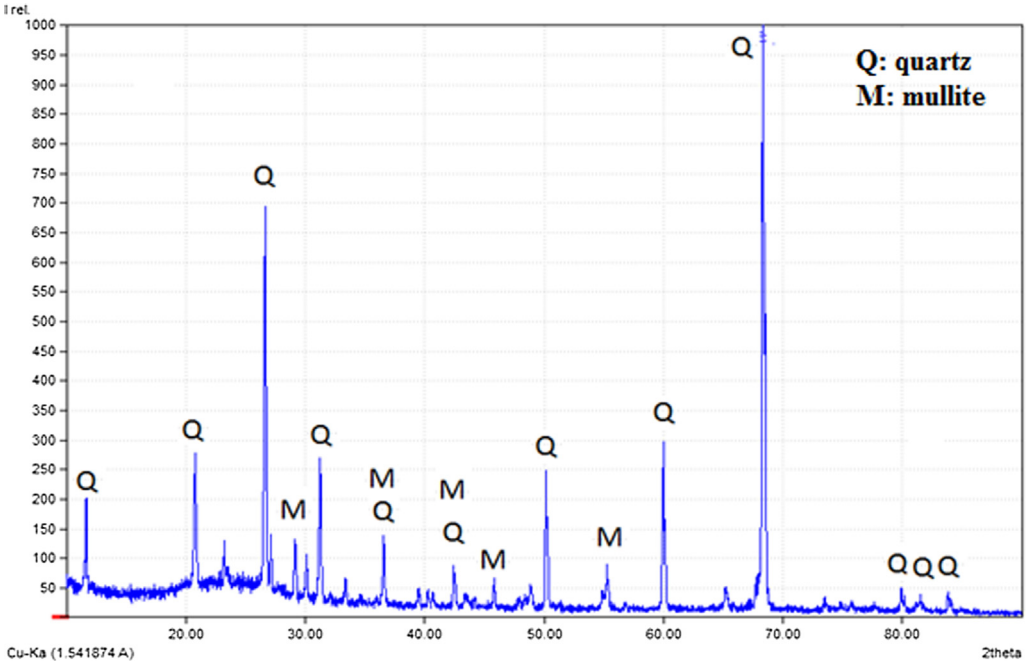

Fig. 15. XRD patterns for 10C geopolymer samples −300 °C - after exposure.

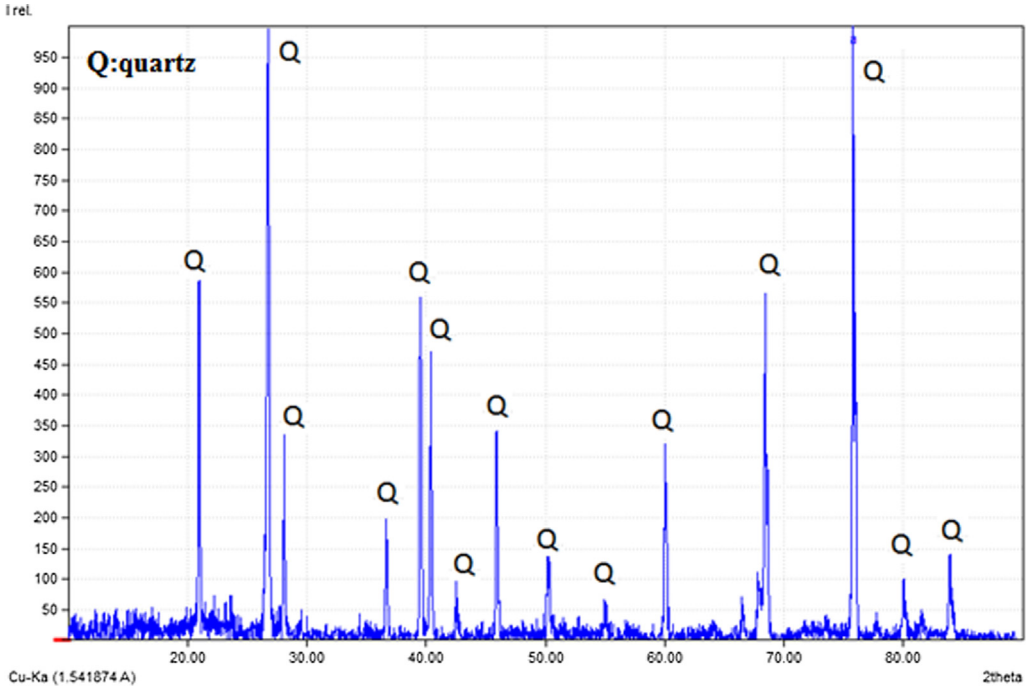

Fig. 16. XRD patterns for 20 SF geopolymer samples −300 °C – after exposure.

temperature [126]. XRD has been applied to investigate the composition of the reaction products formed in geopolymer composites. Figs. 15–18 show the XRD spectra of 10 C and 20 SF geopolymer samples exposed to high temperatures of 300 and 600 °C. A broad hump shows the formation of geopolymerization amorphous gels with 20–40° 2-theta [127]. The consistent appearance of the broad hump at 300 °C showed the composites' thermal resistance properties. New crystalline phases are produced while the samples represent their original structural properties at 300 °C. Some characteristic peaks observed in the XRD model are quartz, thomsonite, zeolite, goethite, and semi-crystalline hillebrandite. For 10 C samples exposed to 300 °C the quartz peaks occurred at 28° and

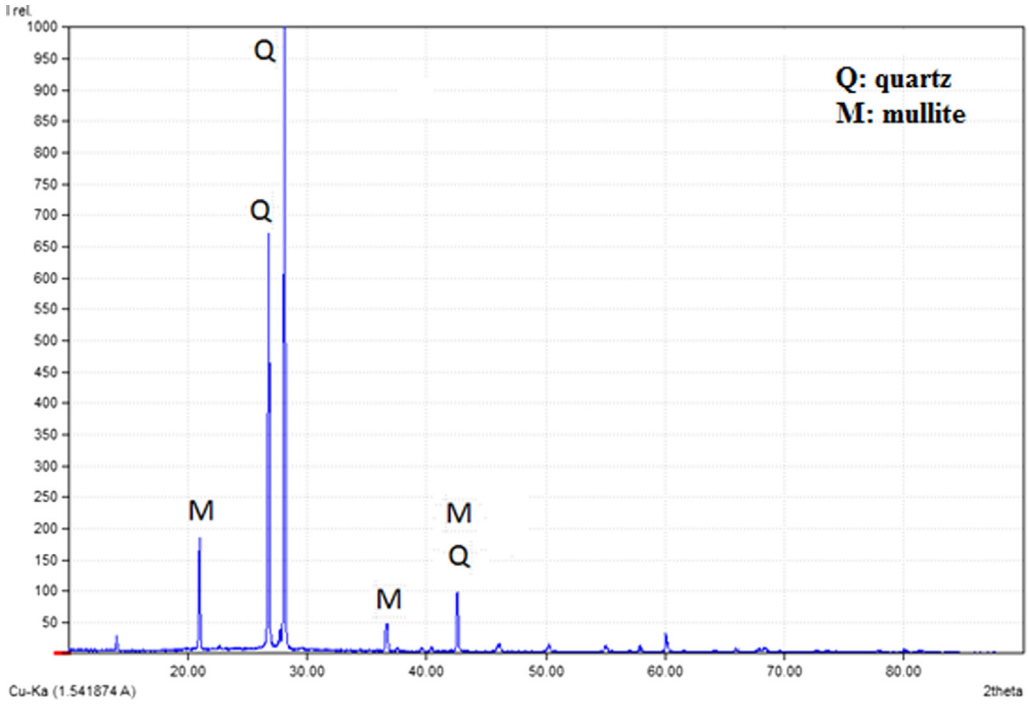

Fig. 17. XRD patterns for 10C geopolymer samples –600 °C – after exposure.

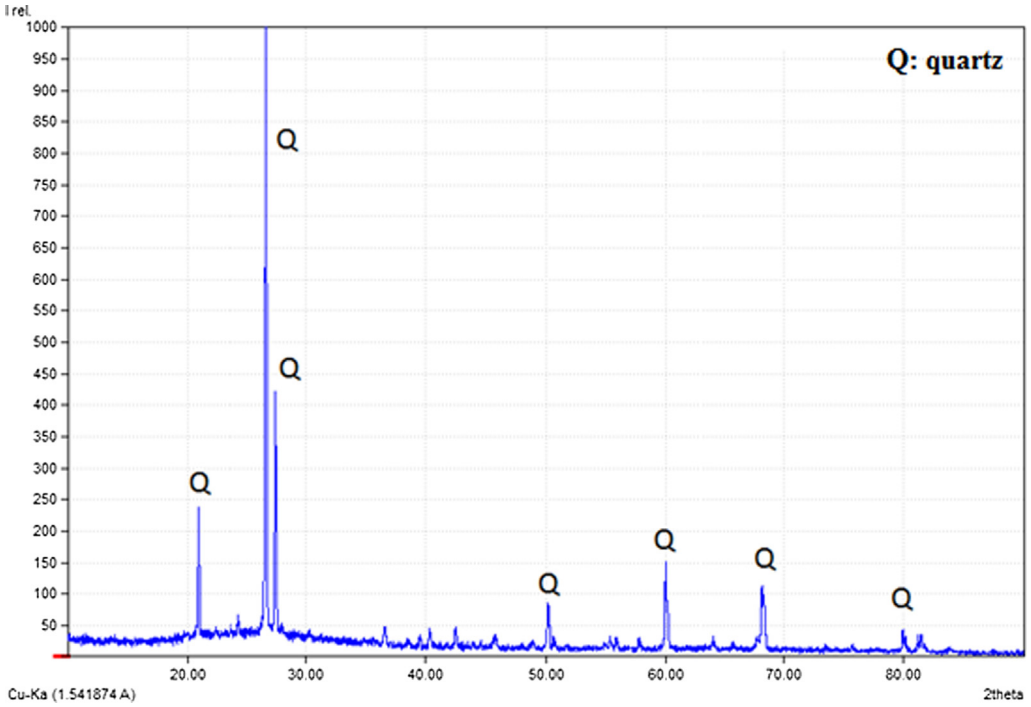

Fig. 18. XRD patterns for 20 SF geopolymer samples (600 °C) – after exposure.

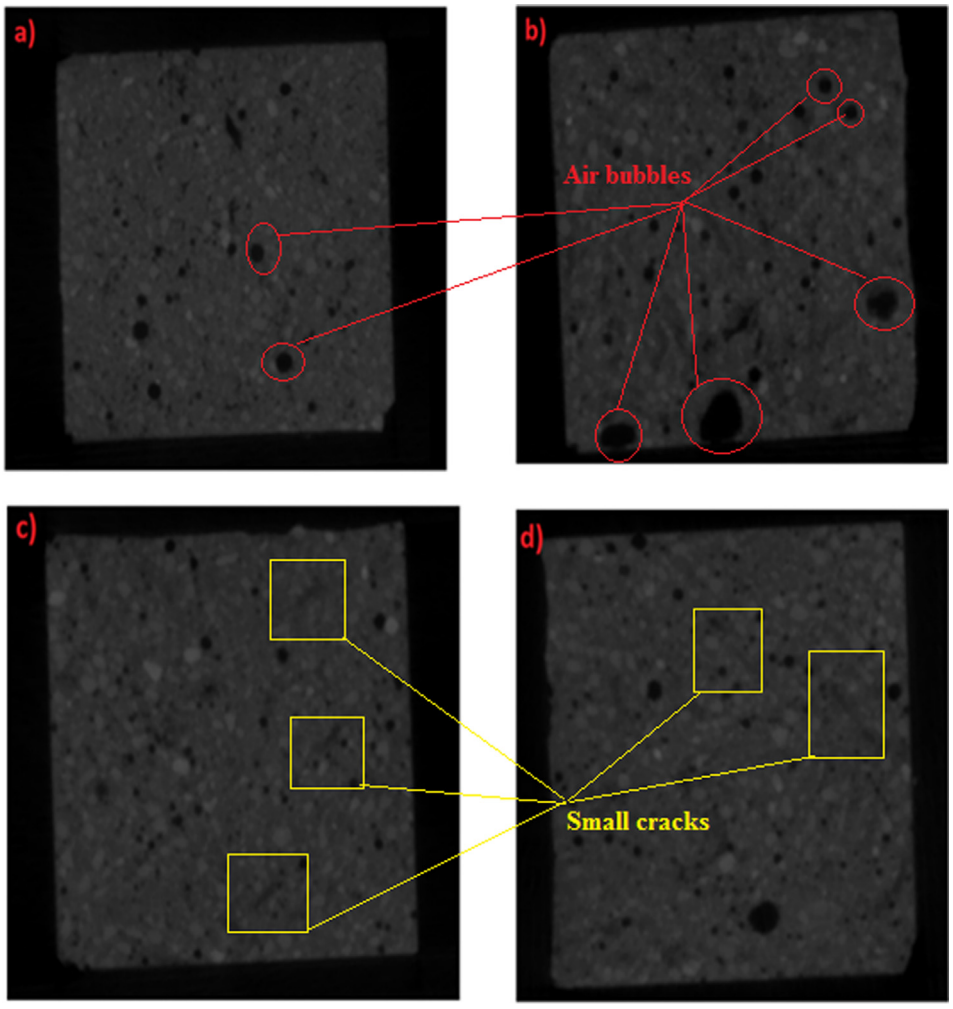

Fig. 19. X-ray CT images for a) 10C sample after exposure to 300 °C b) 10C sample after exposure to 600 °C c) 20SF sample after exposure to 300 °C d) 20SF sample after exposure to 600 °C.

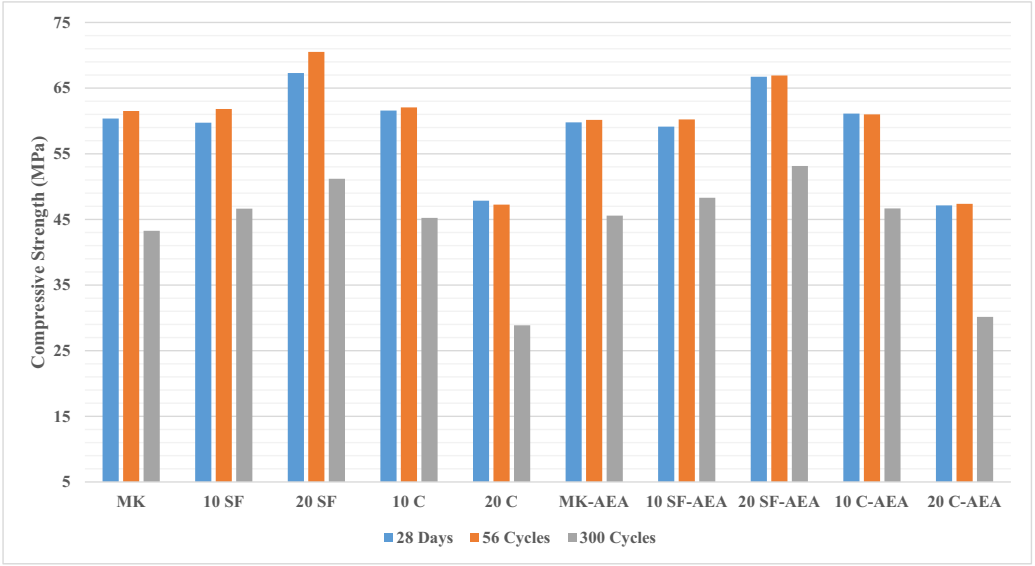

Fig. 20. Residual compressive strength results after freezing-thawing tests.

68° and for 20 SF samples at 28° and 76°. The fact that geopolymer samples have better thermal stability and durability is attributed to their zeolite-like structure [88]. The different types of characteristic peaks may depend on the geopolymer composite mixture designs, aluminosilicate source type, filler type, alkali activator type, unreacted alumina or silica, and other unreacted impurities [128]. At 600 °C, amorphous hump covering quartz peaks at 28° in both 10 C and 20 SF samples were preserved, indicating that these phases were inert during high-temperature exposure [125]. The results showed that geopolymers still had structural stability at 300 °C; however, higher temperatures (600 °C) caused structural problems resulting from the degradation of mechanical properties. Furthermore, the shifting of the amorphous hump to lower angles after 500 °C indicated that in geopolymers, there was a microstructural reconstruction associated with the rearrangement or flow of atomic species such as Si and Al [125].

Therefore, it can be concluded that decomposition of gel, thermal incompatibility, and crystallization result in a decrease in strength in mortars that are subjected to a high-temperature effect of 600 °C in bulk. The geopolymers' structure includes tetrahedral AlO_4 and SiO_4 units randomly distributed along polymeric chains, interconnected spaces of sufficient size to accommodate alkali ions and weakly bound water molecules [129]. Therefore, if this structure is maintained at temperatures above 500 °C, the water molecules held in the cavities suddenly reach high kinetic energy. When there is an increase in the movement of molecules, the held water begins to escape from the structure in the form of steam creating a high internal pressure that produces expansive forces within

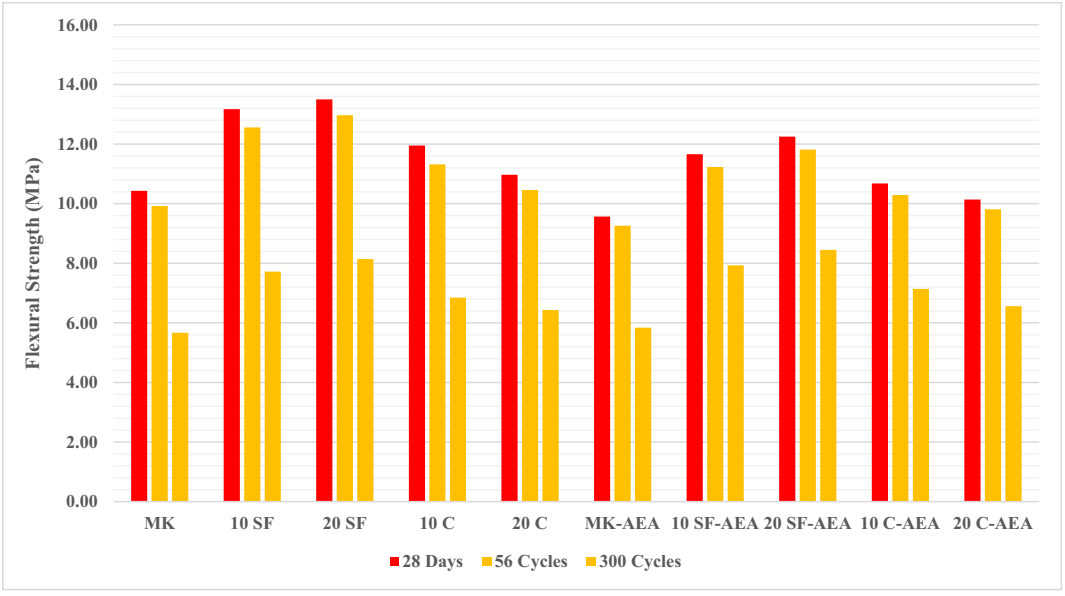

Fig. 21. Residual flexural strength results after freezing-thawing tests.

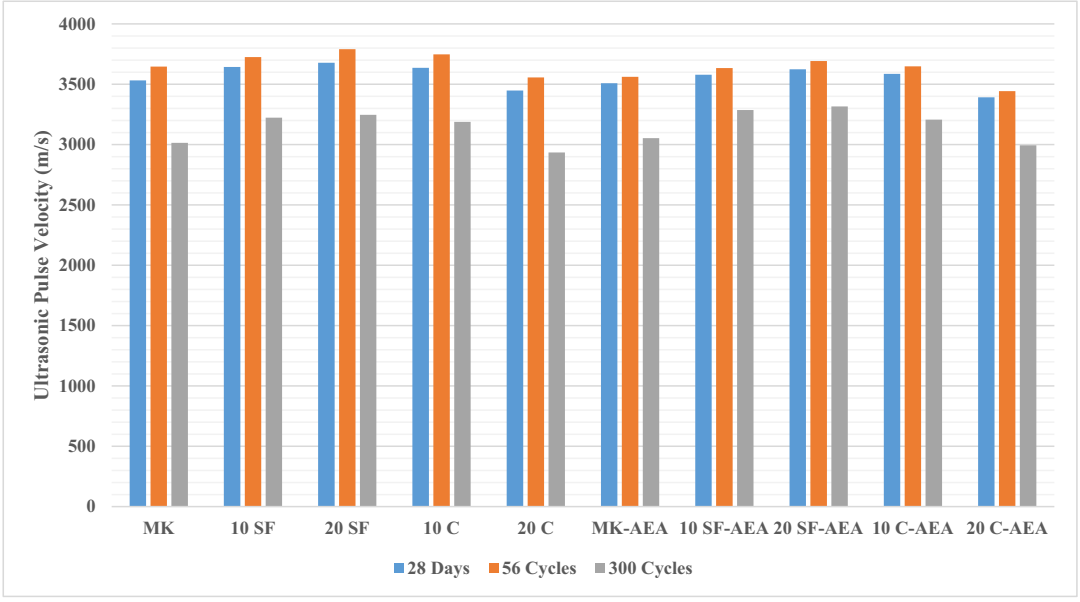

Fig. 22. Ultrasonic pulse velocity results after freezing-thawing tests.

microstructures. Internal and surface cracking occurs in the samples due to the forces generated and the degradation of the microstructures caused by displacement of the hump in XRD models results in the geopolymeric network partial collapse [130].

X-ray CT images of 10C and 20SF samples after exposure to 600 and 900 °C are shown in Fig. 19. Fig. 19 is a representative cross-sectional view of the samples. Due to the drying shrinkage, small cracks are observed near the surface side of the sample. In addition, the temperature gradient in the sample is another cause of crack formation. Particularly during the period in which water evaporation increases, a lower temperature is formed in the core area of the sample than the outside. Because of this, the shrinkage in the core area is less than the outer layer. This mismatch between shrinkage creates cracks. In addition, the size and water content of the sample can trigger crack formation. In terms of crack formation, the 10C sample will experience higher strength degradation than the 20SF sample due to cracks caused by the temperature effect of 600–900 °C. In X-ray CT images, bright colors show components such as gravel and fine aggregate with high X-ray attenuation, while components with none X-ray attenuation or low are indicated by dark colors (air voids). In addition to the small cracks in the internal structures, the morphological structures of the geopolymers have rounded pores. A more dense structure was observed in the 20SF sample due to the property of silica fume. In contrast, many more pores were observed in the 10C sample exposed to 900 °C. This result shows that silica fume reduces the loss of strength in the geopolymer sample according to colemanite waste [131–133].

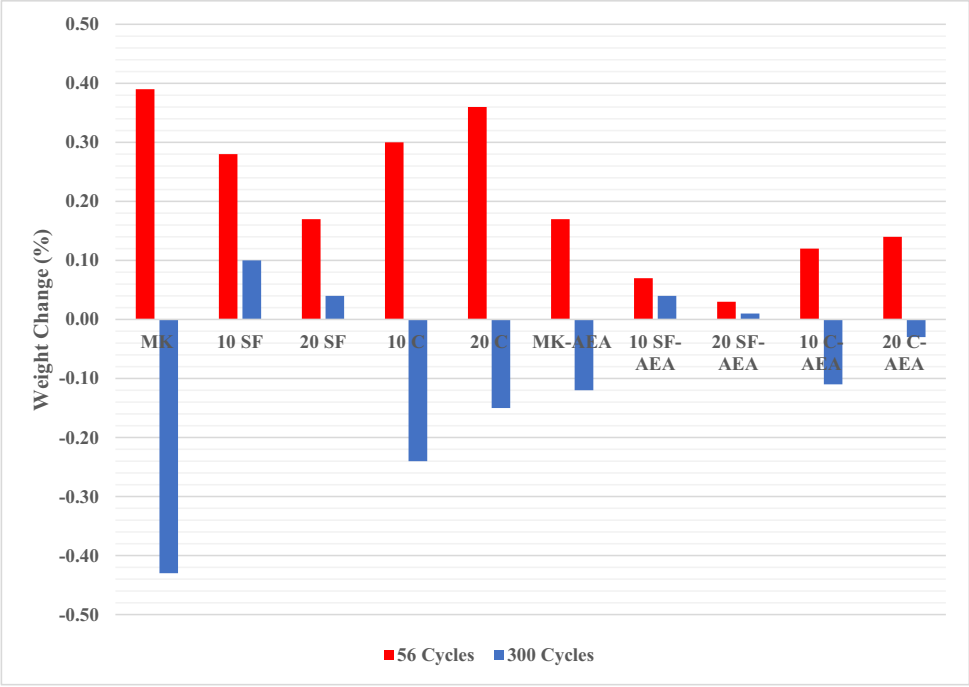

Fig. 23. Weight change rate results after freezing-thawing tests.

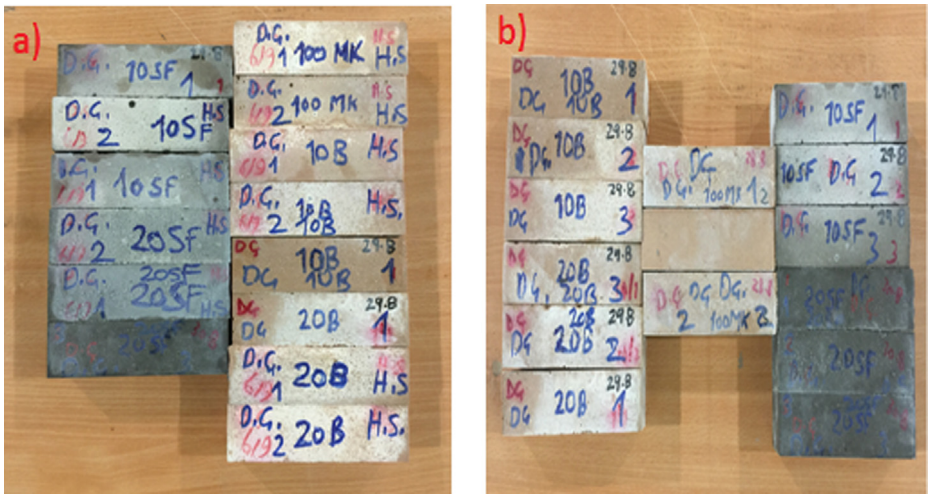

Fig. 24. Geopolymer samples after 56 cycles freezing-thawing test a) without AEA b) with AEA.

3.2. Freezing-thawing test

3.2.1. Compressive and flexural strength and ultrasonic pulse velocity results

The use of air-entraining admixture has shown a reducing effect on the compressive and flexural strengths and ultrasonic pulse velocity results. This has been reported to result from a decrease in pore volume. This is related to workability. The use of air-entraining additives increases the workability and therefore reduces the pore volume. The presence of air voids is effective here. Due to the adverse effect of air content on strength results, strength decreased [134]. For this reason, AEA should be used carefully on applications. This was seen when 28-day results were compared. Compressive strength of 61.59 MPa, flexural strength of 11.95 MPa and ultrasonic pulse velocity of 3636 m/s results were obtained in 28 days for 10C sample, while compressive strength of 61.12 MPa, flexural strength of 10.68 MPa and ultrasonic pulse velocity of 3586 m/s were obtained in 28 days for 20C-AEA samples. Compressive strength of 67.3 MPa, flexural strength of 13.50 MPa and ultrasonic pulse velocity of 3678 m/s results were obtained for 20 SF samples in 28 days while 20 SF-AEA samples had a compressive strength of 66.73 MPa, flexural strength of 12.25 MPa and ultrasonic pulse velocity of 3624 m/s in 28 days. Using air-entraining admixture increased the air content in the mortar, resulting in a decrease in compressive and flexural strength and ultrasonic pulse velocity values. Geopolymer mortar samples showed some loss of strength due to this situation.

The results obtained from the freezing-thawing tests were compared with the results of 28-day results (Figs. 20–22). In this study, trends of compressive strength results were different for two different cycles. It is noteworthy that the compressive strength results of geopolymer mixtures exhibited an increase rather than a reduction for 56 cycles. The humid environment in which the experiment was performed provided the filling of the voids in the samples. This was mainly related to the fact that the geopolymeric matrix was compact, had a good degree of adhesion which made it resistant to the effect of freezing and thawing, in addition, a progress process of the matrix was made through the freezing-thawing cycles. So geopolymeric products are still being created during the 56 cycles of freezing-thawing test. This process can be considered as the continuation of the curing process of geopolymerization. The matrix then gave better results in terms of compressive strength properties and ultrasonic pulse velocity rates. This has been reported by some authors to have contributed to the development of concrete properties (e.g. dynamic modulus and strength) of freezing-thawing cycle tests with the presence of wet and humid ambient conditions [71,135,136]. In these studies, it was thought that activation of raw materials such as fly ash, metakaolin and slag occurred during the test and binding products were formed and frost attack prevented. This phenomenon may not be desirable in determining the freezing resistance of the materials. In order to avoid microstructure changes due to geopolymerization or hydration due to freezing-thawing cycles, it may be reasonable to postpone the test start at raw materials, especially fly ash with low reaction kinetics. When the flexural strength results of geopolymer mixtures were examined, there was a decrease instead of increase in compressive strength. Following the 56 cycle test, the reduction in flexural strength is as follows: When the sample is under the influence of the compressive loads, the cracks are parallel to the compressive load action. It means that the damage is caused by the flexural stress perpendicular to the compressive load. For this reason, the influence of freezing-thawing cycles on flexural strength is greater than compressive strength.

As a result of the 56 cycles of freezing-thawing effect, an increase in compressive strength was also observed in geopolymer samples with air-entraining admixture (AEA), but this was smaller compared to samples without air-entraining. Using AEA allowed the geopolymer samples to remain more stable. The highest compressive strength result after test was 70.52 MPa in 20 SF samples. The lowest value was seen in 20C samples as 47.26 MPa. The highest flexural strength after freezing-thawing test was observed in 20 SF samples as 12.97 MPa. The lowest value was 9.81 MPa in 20C-AE sample. The highest ultrasonic pulse velocity after freezing-thawing test was 3791 m/s in 20 SF samples.

An increase in compressive strength was observed after 56 cycles but a decrease in compressive strength was observed after 300 cycles. At the end of the 300 cycle freezing-thawing test, losses occurred in both strengths' results and ultrasonic pulse velocity. At the end of the test, the highest residual compressive strength was obtained in 20 SF-AEA samples with 53.14 MPa, when the lowest residual compressive strength was obtained with 28.86 MPa in

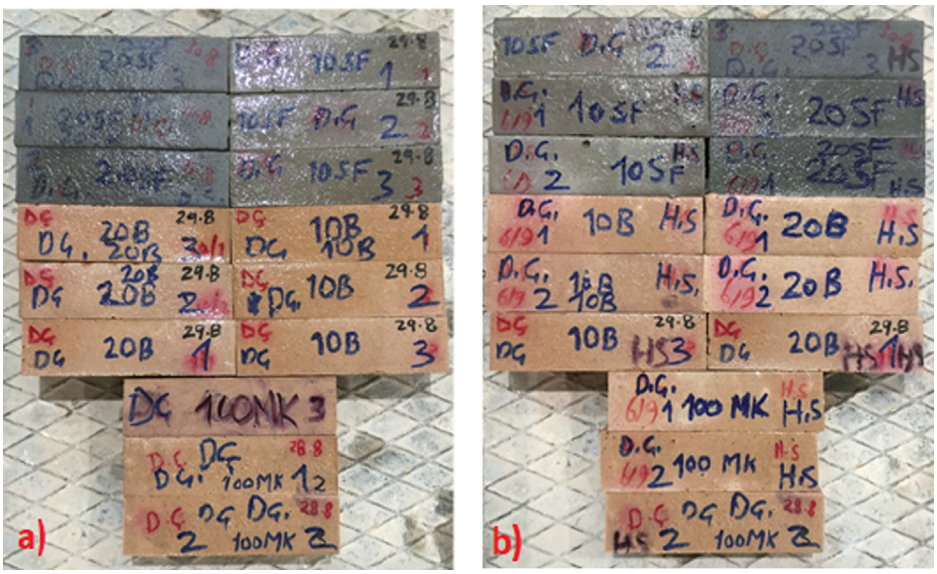

Fig. 25. Geopolymer samples after 300 cycles freezing-thawing test a) without AEA b) with AEA.

20C samples. The highest flexural strength result was obtained in 20 SF-AEA samples with 8.45 MPa and the lowest result was obtained with 5.67 MPa in MK sample. When the UPV results were evaluated, the lowest and highest values after 300 cycles were 2935 m/s and 3316 m/s, respectively. Silica fume, which is a very active pozzolan, has generally been shown to produce satisfactory behavior in the freezing-thawing cycles without the need for a specific air void structure [137]. Also if colemanite waste is replaced with primary binder material up to 10%, it is possible to influence the results positively.

The most critical cause for the breakdown is the water expansion in the mortar which is permeable while freezing occurs. When freezing occurs, the water volume increases by approximately 9% and hydraulic pressure is created in the sample due to this effect [138]. Furthermore, when the available free space is got full, freezing creates hydraulic pressure on the geopolymer matrix surrounding the ice. If the force exceeds the tensile strength of the mortar, the formation of micro-cracks starts and deterioration occurs. It is expected that compressive strength will decrease with this effect [139,140]. Since geopolymer samples have high initial compressive strength, they can withstand higher pressures from freezing water before the formation of micro-cracks. Due to the compact structure present in the geopolymeric matrix, a good adhesion level is achieved. With this effect, geopolymer composites are highly resistant to the effect of freezing-thawing test.

The geopolymer samples thus began to suffer the real distortion effect in subsequent cycles after the freezing-thawing effect, which contributed to geopolimerization in a sense occurring in the first 56 cycles. Because of this, it may be necessary to determine the actual start time of the freezing-thawing test. Reducing the surface stresses caused by the use of air-entraining admixture is provided. It provides a controlled, small, uniformly distributed air bubble in

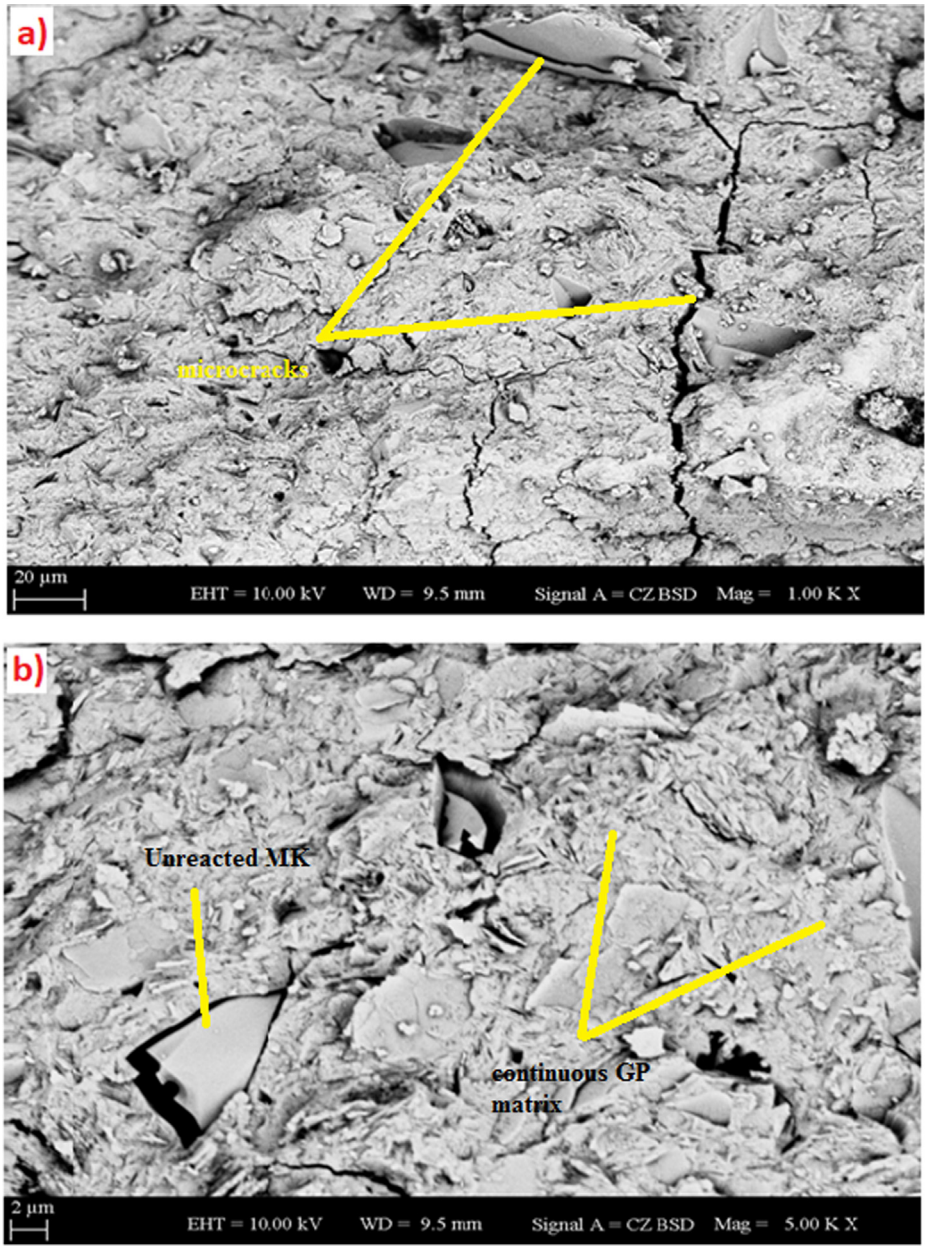

Fig. 26. SEM micrographs of 10 C samples after exposure to freezing-thawing a) magnified 1000 times and b) magnified 5000 times.

the fresh sample, which is permanent even after hardening is complete. This ensures that small air bubbles remain in the concrete. This provides resistance to the effect of freezing-thawing [134]. The air-entraining admixture has been found to reduce the rates of reduction in compressive and flexural strengths and ultrasonic pulse velocity results after the freezing-thawing effect begin to manifest itself. The residual strength results due to these conditions were higher.

3.2.2. Weight change and visual inspection of the samples

The percentages of weight changes obtained as a result of freezing-thawing tests are given in Fig. 23. The moist environment ensured where the test has conducted the filling of the voids in the samples produced and therefore the weights increased in the geopolymer samples after 56 cycles. The increase rates decreased in the case of using AEA. In this case, since using AEA increased the air-bubble voids, the weight increase was limited. The highest weight increase in geopolymer samples was observed in MK sample as 0.39% and the lowest weight increase was observed in 20 SF-AE as 0.03% after 300 cycles freezing-thawing test [141]. According to the MK sample, silica fume and colemanite waste replacement decreased weight changes. Silica fume and colemanite waste can act similarly in case of substitution and reduce the voids ratio to form a more compact structure. So weight change results were lower with silica fume and colemanite in the geopolymer composites [81].

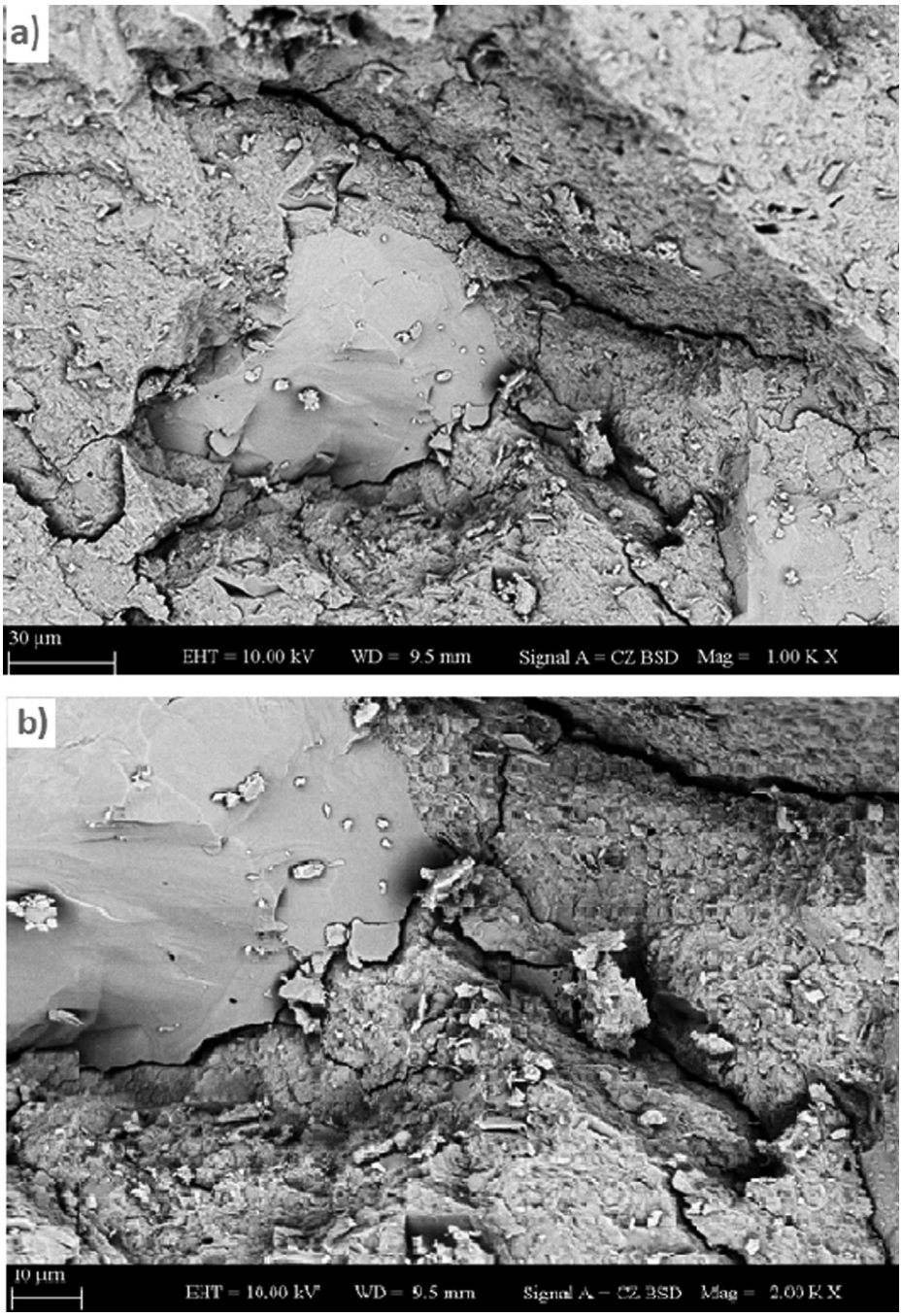

Fig. 27. SEM micrographs of 20 SF samples after exposure to freezing-thawing a) magnified 1000 times and b) magnified 2000 times.

This situation, which occurred in 56 cycles, started to change with the progressing cycles. However, after 300 freezing-thawing cycles, no striking reduction in weight of the samples was observed. The weight change that occurs during the freezing-thawing cycles is due to the movement of moist media outside and inside the sample and micro-cracks. As soon as micro-cracks occur, filling the degraded zones with the effect of the surrounding moist environment will increase the weight of the sample. Because of this, weight gain was observed in the first 56 cycles freezing-thawing test. Weight loss was observed due to desquamation on the surface of the sample with progressing cycles. However, the compact structure of the geopolymer sample has led to this occurrence at a low rate. Because of this, weight loss was also low. Due to the natural structure of the silica fume, weight reduction was not seen, but the weight increase according to the 56 cycles decreased. The air-entraining additive reduced weight loss. The

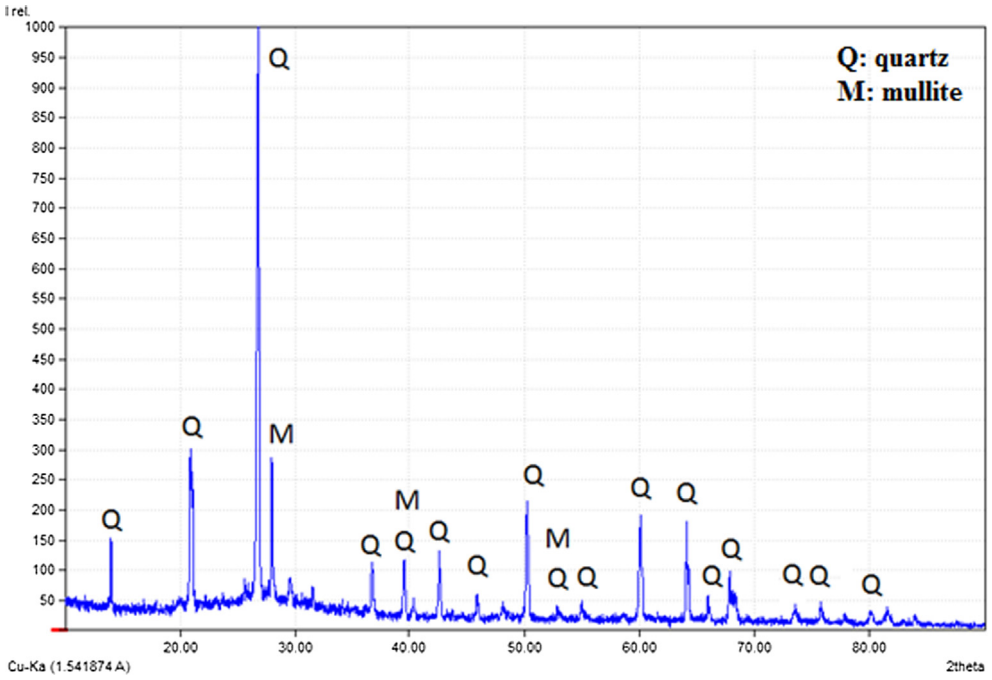

Fig. 28. XRD patterns for 10 C geopolymer samples after exposure to freezing-thawing.

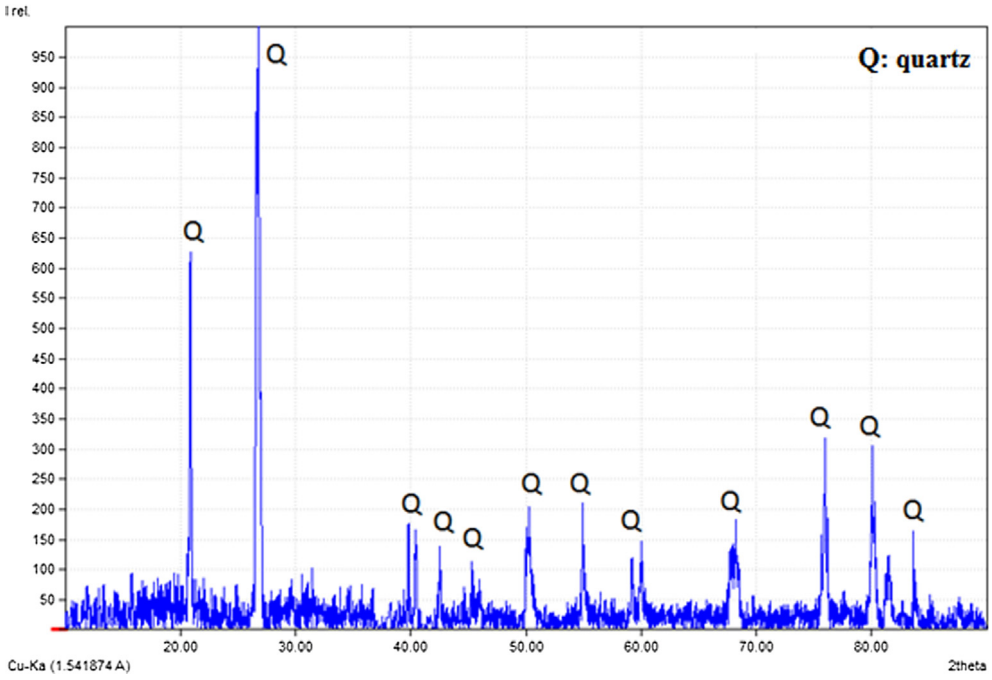

Fig. 29. XRD patterns for 20 SF geopolymer samples after exposure to freezing-thawing.

stable, homogeneous porous network obtained by the addition of an air-entraining additive limited the weight loss change [142,143]. The highest weight loss in geopolymer samples was observed in MK sample as 0.43% and the lowest weight increase was observed in 20 SF-AE as 0.01% after 300 cycles freezing-thawing test.

After the freezing-thawing cycles were completed, all surfaces of the geopolymer samples were carefully examined. Surface analysis after 56 cycles and 300 cycles of freezing-thawing tests showed no significant damage to the appearance of the samples. No significant change in external appearance was observed, while the deterioration remained at the microcrack level. The main reason for the deterioration in the water expansion formed in the permeable structure. With freezing, water expands to 9% and leads to the formation of hydraulic pressure. This results in micro-cracks. However, this did not lead to surface damage. Visual inspection of samples after 56 and 300 cycles is given in Figs. 24, 25 [144].

Microstructural changes in 10 C and 20 SF samples after the freezing-thawing effect of 300 cycles are shown in Figs. 25, 26. Microcracks formation was observed when the SEM images of the geopolymer samples were examined. Most of them pass through the existing interface between the metakaolin spheres and the gel, indicating that the interface has a defective area. It was also observed that the microcracks were interconnected to form a network. A small amount of damage to the integrity of the structure can be explained in this way. This explains the losses in compressive and flexural strengths and ultrasonic pulse velocity results. However, it was observed that the geopolymer sample remained stable due to the slow development of microcracks. Because of this, it has been observed that geopolymer samples

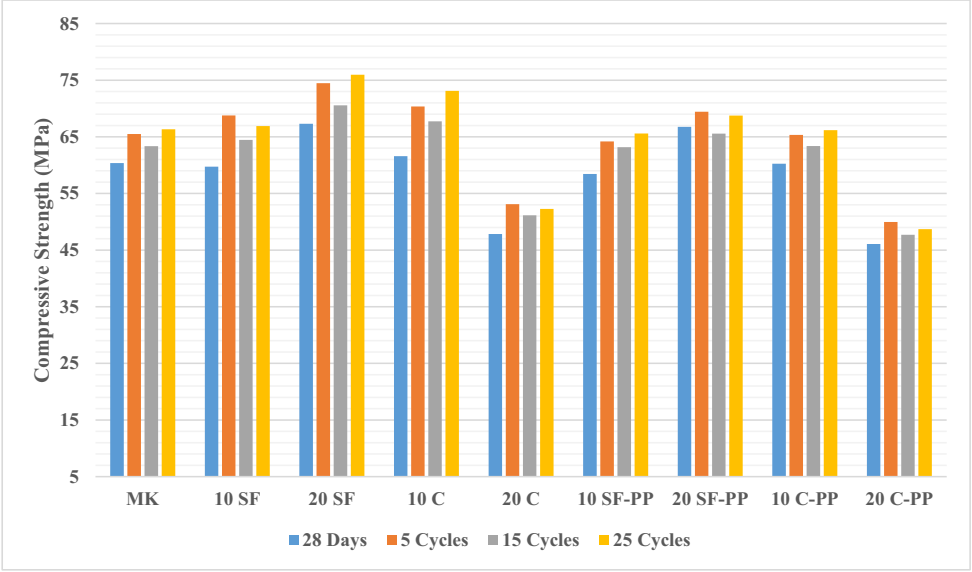

Fig. 30. Residual compressive strength results after wetting-drying tests.

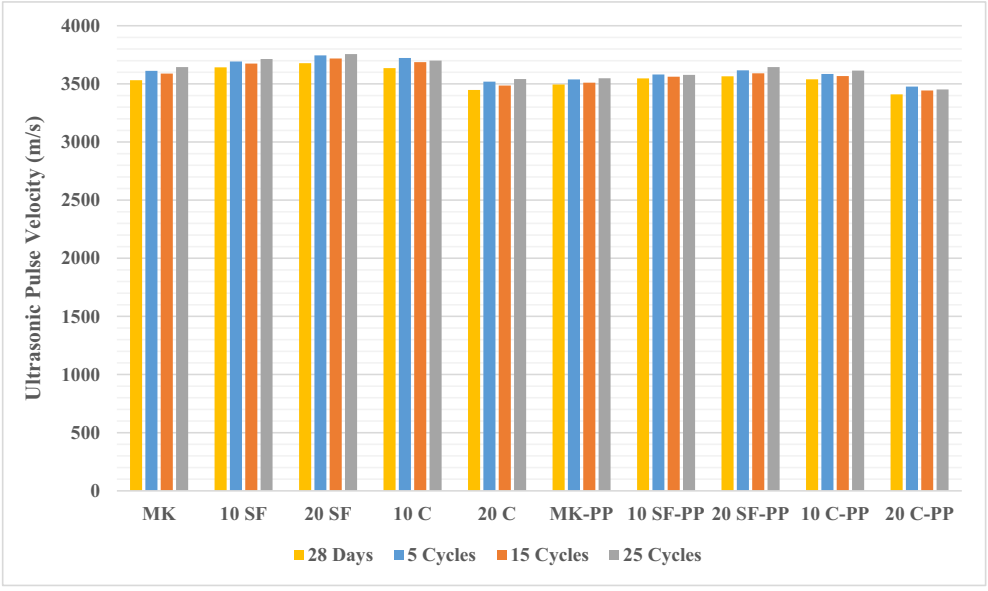

Fig. 31. Residual ultrasonic pulse velocity results after wetting-drying tests.

showed high resistance against the freezing-thawing effect of 300 cycles. The results obtained are consistent with other studies just as shown in Fig. 27 [138,145].

XRD tests were performed to investigate the polymerization products of the geopolymer and to perform compound analyzes. After the 300 cycles of freezing-thawing test, XRD spectra of 10C and 20 SF samples between 10°–80° 2θ were examined and partial gel dissolution and further gel development were observed in the geopolymers. For 10C and 20 SF samples were exposed to freezing-thawing, quartz peaks were formed at 22° and 28°. Different characteristic quartz peaks could not be detected from the rest of the diffraction angles. The main crystals seen in geopolymer samples after freezing-thawing test are quartz and mullite. Since fine aggregate is proportionally the main component in the mortar, quartz is the main phase seen in the XRD analysis. The hump formed between 20° –40° 2θ shows the typical XRD pattern of geopolymer amorphous gel. Some low quartz peaks were detected at higher angles, but these did not affect the main stability of the geopolymer samples. So, according to the XRD patterns, no significant change was observed in peaks in comparison with the pretreatment states of 10C and 20 SF samples under the freezing-thawing effect (Figs. 28, 29). The results obtained are consistent with previous results [146].

3.3. Wetting-drying test

During the formation of wetting-drying cycles, fluctuations were observed in the compressive strength, ultrasonic pulse veloc-

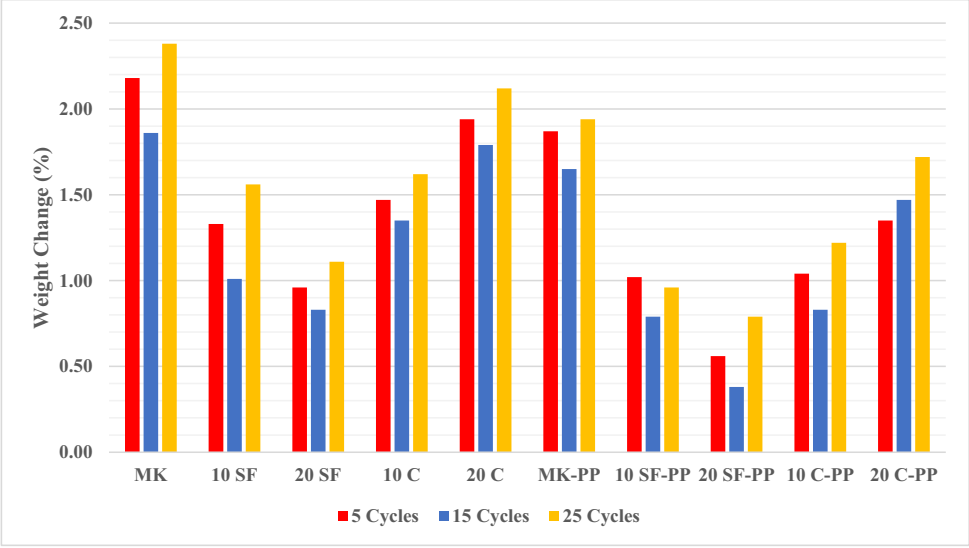

Fig. 32. Weight change rate results after wetting-drying tests.

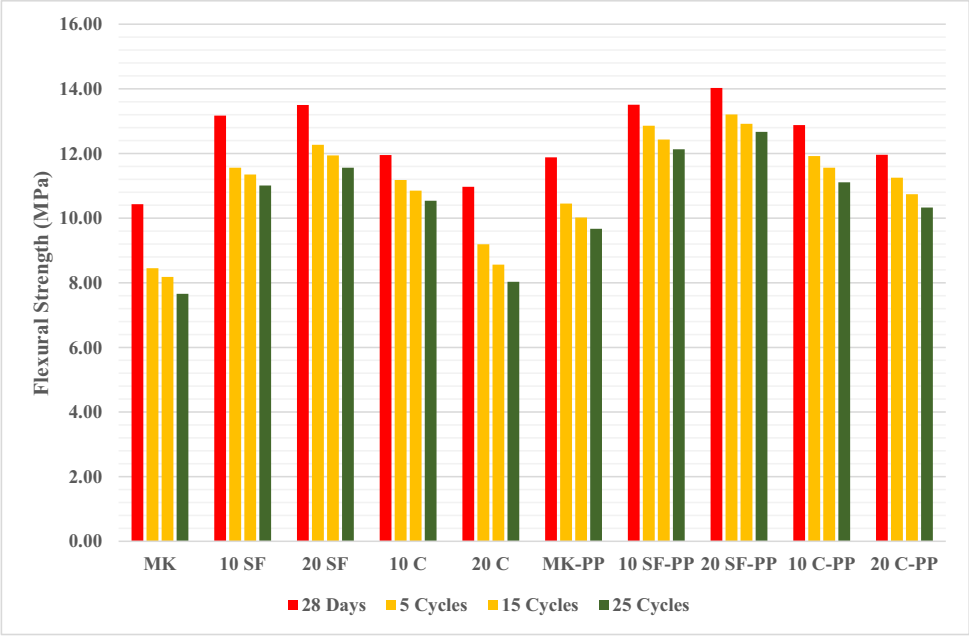

Fig. 33. Residual flexural strength results after wetting-drying tests.

ity, and weight changes' results by applying heating-cooling cycles. If the results were analyzed in general, an increase in the results after 5 cycles, a decrease in the results after 15 cycles and an increase again in the results after 25 cycles were seen. These fluctuations in the compressive strength, ultrasonic pulse velocity, and weight changes' results are expected and are attributed to the severity of the regime which undermines the integrity of the composite materials under service conditions. With the formation of heating-cooling cycles with wetting-drying; in fact, the repetitive crystallization of ions in water by continuous repetition of hydration and evaporation creates some changes in the composite material; this leads to shrinkage following expansion and creates internal stresses in the pores which increase or decrease the strength of the composite material. In other words, drying shrinkage and thermal expansion coefficient differences are the main reason for this situation [52,147].

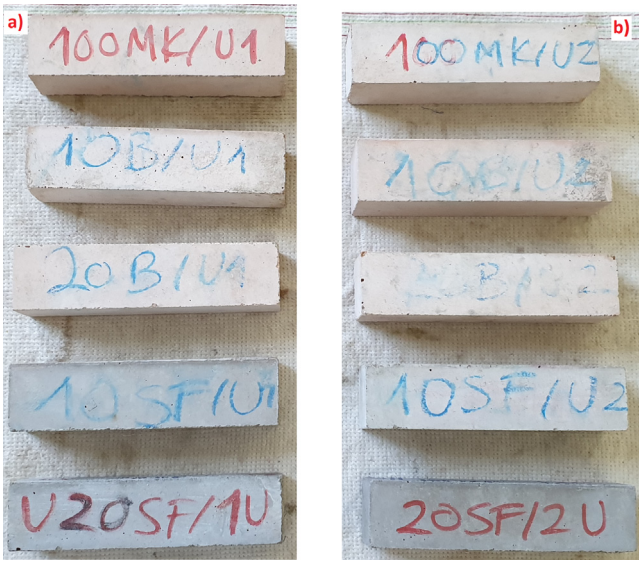

Fig. 34. Geopolymer samples after 25 cycles wetting-drying test a) without PP b) with PP.

In addition, the density of the mortar is further increased by heating the sample under the influence of wetting-drying, and thus the UPV results are higher. This is due to the fact that geopolymerization is faster and complete. Therefore, it has been shown in different studies that wetting-drying method can be used as a curing method. Petermann et al. [148] found the highest strength and lowest porosity for the mortar when applied wetting-drying to the geopolymer samples as a curing method. This showed that in the first stage more geopolymerization occurred with wetting curing and in the next stage higher compressive strength was achieved by drying curing. Hydration reactions of high-calcium compounds are supported by wetting curing while strengthening is supported by providing geopolymer structure containing improved bond with heat curing. Therefore, wetting-drying method has been determined as the most suitable method as a curing method by Arslan et al. According to Arslan et al., with the wetting-drying curing, the geopolymerization's formation and the new crystalline geopolymerization products' formation were provided [144].

The compressive strength results of the 10 C sample were 70.36 MPa after 5 cycles, 67.74 MPa after 15 cycles and 73.12 MPa after 25 cycles. The compressive strength results of 20 SF samples were 74.47 MPa after 5 cycles, 70.56 MPa after 15 cycles and 75.97 MPa after 25 cycles (Fig. 30). The ultrasonic pulse velocity results in the 10 C sample were 3723 m/s after 5 cycles, 3687 m/s after 15 cycles, and 3701 m/s after 25 cycles. In 20 SF samples, UPV results were 3745 m/s after 5 cycles, 3718 m/s after 15 cycles and 3756 m/s after 25 cycles (Fig. 31). With respect to polypropylene fibers, the decrease in compressive strength is caused by both the low density of the fibers used and the flocculation of the fibers resulting in a decrease in ultrasonic pulse velocity

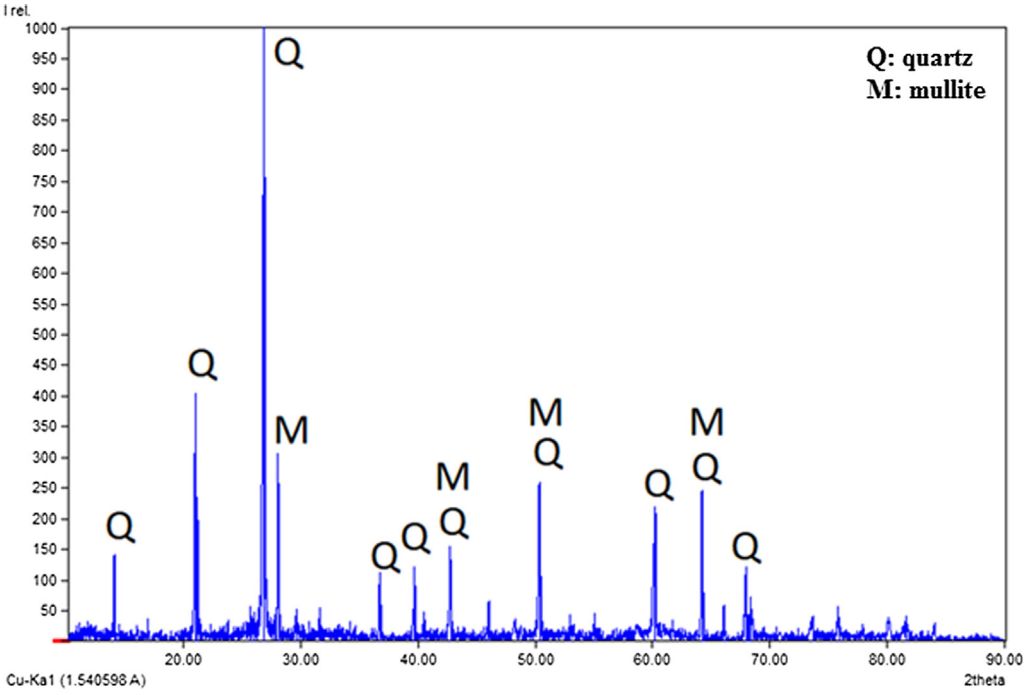

Fig. 35. XRD patterns for 10 C geopolymer samples after exposure to wetting-drying.

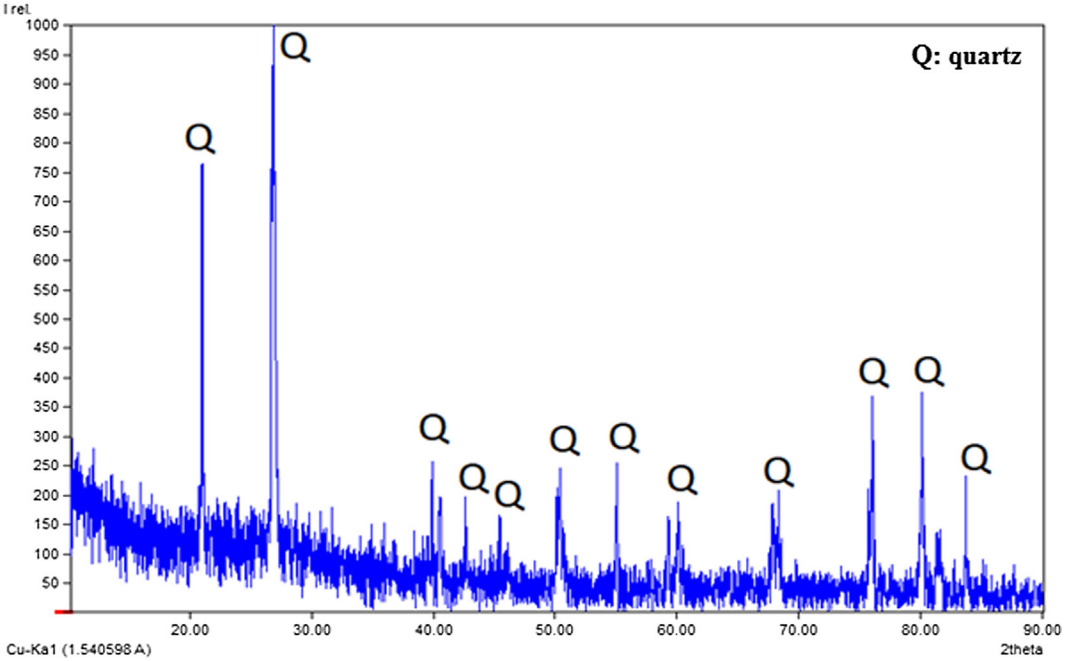

Fig. 36. XRD patterns for 20 SF geopolymer samples after exposure to wetting-drying.

and compressive strength and an increase in water absorption rate. According to this; it was observed that compressive strength and ultrasonic pulse velocity values decreased with polypropylene fiber additive in all blends [99]. The compressive strength results of 10 C-PP samples were 65.35 MPa after 5 cycles, 63.38 MPa after 15 cycles and 66.18 MPa after 25 cycles. The compressive strength results of 20 SF-PP samples were 69.44 MPa after 5 cycles, 65.56 MPa after 15 cycles and 68.75 MPa after 25 cycles. The ultrasonic pulse velocity results in 10 C-PP samples were 3585 m/s after 5 cycles, 3567 m/s after 15 cycles, and 3614 m/s after 25 cycles. In 20 SF-PP samples, UPV results were 3617 m/s after 5 cycles, 3591 m/s after 15 cycles and 3645 m/s after 25 cycles.

When the weight changes according to the initial situation were examined, the weight changes after 5,15 and 25 cycles in the 10 C sample were 1.47%, 1.35%, and 1.62%, respectively. In 20 SF samples, the weight changes after 5, 15 and 25 cycles were 0.96%, 0.83% and 1.11%, respectively. In addition to the low modulus that causes low residual stress, polypropylene fibers have been found to be hydrophobic, meaning that they desire to move away from water-based systems [100,101]. Because of this, weight changes were less due to the effect of polypropylene fibers. When the weight changes according to initial situation were examined, the weight changes after 5,15 and 25 cycles in the 10 C-PP samples were 1.04%, 0.83% and 1.22%, respectively. In 20 SF samples, the weight changes after 5,15 and 25 cycles were 0.56%, 0.38% and 0.79%, respectively (Fig. 32).

When the flexural strength results of geopolymer mixtures were examined, there was a decrease instead of an increase in compressive strength. The reduction in flexural strength is as follows: When the sample is under the influence of the compressive loads, the cracks are parallel to the compressive load action. It means that the damage is caused by the flexural stress perpendicular to the compressive load. Therefore, the effect on flexural strength is greater than compressive strength for wetting-drying. Due to this situation, a decrease in flexural strength was observed with oncoming cycles. The flexural strength results in the 10 C sample were 11.18 MPa after 5 cycles, 10.85 MPa after 15 cycles and 10.54 MPa after 25 cycles. In 20 SF samples, the flexural strength results were 12.27 MPa after 5 cycles, 11.94 MPa after 15 cycles and 11.56 MPa after 25 cycles. Polypropylene fibers can control the cracks formed while reducing the width and number of cracks. This is the main reason for the increase in flexural strength. The positive behavior of the fibers in flexural strength in concrete can be explained by the fiber's short distance and a very large connection in the matrix. Thus, the results in polypropylene reinforced samples were higher. The flexural strength results in the 10 C-PP samples were 11.92 MPa after 5 cycles, 11.56 MPa after 15 cycles, and 11.11 MPa after 25 cycles. In 20 SF-PP samples, the flexural strength results were 13.21 MPa after 5 cycles, 12.92 MPa after 15 cycles and 12.67 MPa after 25 cycles (Fig. 33).

According to the visual inspection after the 25 cycles wetting-drying test, geopolymer mortars remain structurally stable without any visible cracks or deterioration on their surfaces. Obviously, there was no significant damage to the appearance of the geopolymer mortar samples after 25 cycles of wetting-drying, while the deterioration remained at the level of micro-cracks (Fig. 34).

XRD analyses of 10 C and 20 SF are given in Figs. 35, 36. When the XRD patterns are examined, the crystal peaks are defined as quartz. Quartz, together with mullite, represents the majority of peaks observed in the diffraction image. In addition, broad hump representing the typical amorphous geopolymer gel phase between 22° and 28° 2θ was detected in two samples [81]. Although some small shiftings were observed in the location of the peaks in both samples, no significant differences were observed. This shows that the system maintains its structure under the effect of wetting-drying and the geopolymer reaction has begun to be rearranged. The microstructural changes in the 10 C and 20 SF samples after the wetting-drying effect of 25 cycles are shown in Figs. 36, 37. Significant differences were not observed when geopolymer samples' SEM images were examined after wetting-drying. Therefore, it was observed that geopolymer samples showed high resistance to wetting-drying effect

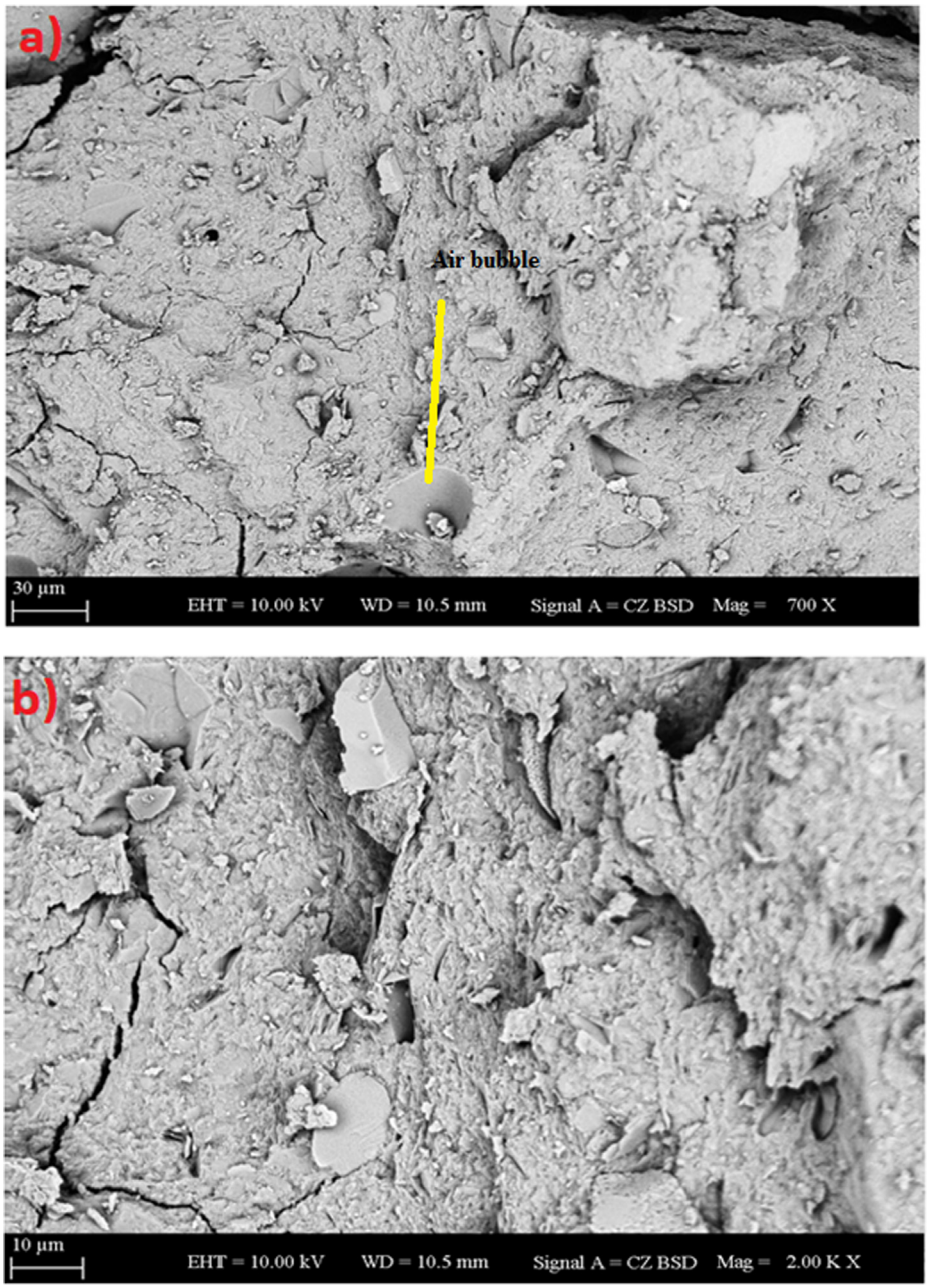

Fig. 37. SEM micrographs of 10 C samples after exposure to wetting-drying a) magnified 700 times and b) magnified 2000 times.

consisting of 25 cycles. When the micrographs of the 10 C sample are examined, the continuity of the geopolymer matrix is clearly evident, so it has been found that the use of colemanite waste in the geopolymeric system creates a good degree of binding to the wetting-drying effect. Similarly, 20 SF samples (Figs. 27 and 38) have been found to have a consistent and compact matrix resulting from the property of silica fume after wetting-drying effect [149].

4. Conclusions

In this study, the durability properties of the samples formed in the case of colemanite waste and silica fume substitution to geopolymer matrices produced using metakaolin as the main binding material were investigated:

- The compressive and flexural strengths of geopolymer composites were significantly reduced by a temperature range of 600 °C to 900 °C due to the dehydration of the geopolymer matrix, the melting of the fibers due to high temperature and the thermal reaction mechanism of free water evaporation. The decrease in flexural strength was higher than compressive strength with high-temperature effect. This was due to the fact that the flexural strength was more sensitive to the development of internal microstructure defects, such as the propagation of cracks and the growth of porous structures at high temperatures.
- When compared to the normal non-fibrous ones, the specimens with Polypropylene fibers yielded a slight enhancement to the performance of the manufactured composites.
- The replacement of SF up to %20 and colemanite waste up to 10% increased the residual compressive and flexural strengths.

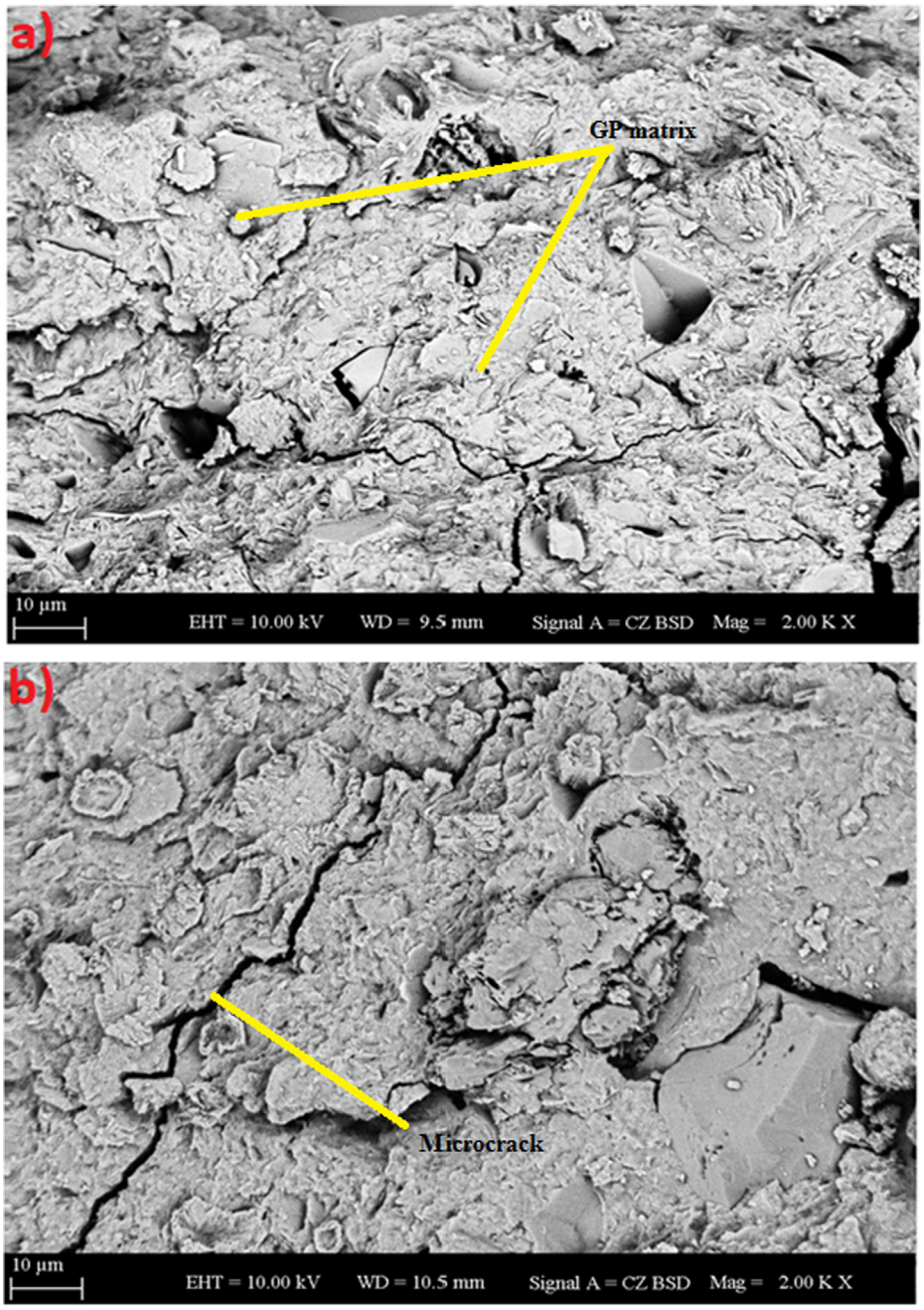

Fig. 38. SEM micrographs of 20 SF samples after exposure to wetting-drying a) magnified 2000 times and b) magnified 2000 times.

- With a significant loss of compressive strength in the 600 °C–900 °C range, cracks have started to be seen. After 900 °C, geopolymer samples had a significant amount of color change, but the cracks remained at a lower rate. This was consistent with the fact that geopolymer specimens maintained stable conditions under the high-temperature effect.
- The use of air-entraining admixture has shown a reducing effect on the results of compressive and flexural strengths and ultrasonic pulse velocity. The use of air-entraining additives increases the workability and therefore reduces the pore volume. Due to the adverse effect of air content on strength results, strength decreased.
- Under the effect of 56 cycles freezing-thawing test, it is noteworthy that the compressive strength results of geopolymer mixtures exhibited an increase rather than a reduction. The humid environment provided in which the experiment was performed filling of the voids in the produced samples and thus increased ultrasonic pulse velocity rates.
- An increase in compressive strength was observed after 56 cycles but a decrease in compressive strength was observed after 300 cycles. At the end of the 300 cycle freezing-thawing test, losses occurred in the compressive and flexural strengths and ultrasonic pulse velocity results.
- During the formation of wetting-drying cycles, fluctuations were observed in the compressive strength, ultrasonic pulse velocity, and weight changes' results by applying heating-cooling cycles. If the results were analyzed in general, an increase in the results after 5 cycles, a decrease in the results after 15 cycles and an increase again in the results after 25 cycles were seen. These fluctuations in the compressive

strength, ultrasonic pulse velocity, and weight changes' results are expected and are attributed to the severity of the regime which undermines the integrity of the composite materials under service conditions.

Declaration of Competing Interest

The authors declare that they have no known competing financial interests or personal relationships that could have appeared to influence the work reported in this paper.

Acknowledgment

This work was supported by the research fund of the Yildiz Technical University – Turkey, the authors would like to express their sincere gratitude to scientific research coordination unit for their financial support to the project (Project number: 2016-05-01-DOP04).

References

[1] V.M. Malhotra, Introduction: sustainable development and concrete technology, Concr. Int. 24 (7) (2002).
[2] T. Naik, Sustainability of concrete construction, Practice Period. Struct. Design Construct. 13 (2) (2008) 98–103.
[3] Z. Pan, Z. Tao, Y.F. Cao, R. Wuhrer, T. Murphy, Compressive strength and microstructure of alkali-activated fly ash/slag binders at high temperature, Cem. Concr. Compos. 86 (2018) 9–18.
[4] Z. Pan et al., Damping and microstructure of fly ash-based geopolymers, J. Mater. Sci. 48 (2013) 3128–3137.
[5] P. Nath, P.K. Sarker, Effect of GGBFS on setting, workability and early strength properties of fly ash geopolymer concrete cured in ambient condition, Constr. Build. Mater. 66 (2014) 163–171.
[6] G.S. Ryu, Y.B. Lee, K.T. Koh, Y.S. Chung, The mechanical properties of fly ash-based geopolymer concrete with alkaline activators, Constr. Build. Mater. 47 (2013) 409–418.
[7] Biranchi Panda, Cise Unluer, Ming Jen Tan, Investigation of the rheology and strength of geopolymer mixtures for extrusion-based 3D printing, Cem. Concr. Compos. 94 (2018) 307–314.
[8] Biranchi Panda et al., Additive manufacturing of geopolymer for sustainable built environment, J. Cleaner Prod. 167 (2017) 281–288.
[9] Biranchi Panda, Cise Unluer, Ming Jen Tan, Extrusion and rheology characterization of geopolymer nanocomposites used in 3D printing, Compos. B Eng. 176 (2019) 107290.
[10] P.K. Sarker, S. McBeath, Fire endurance of steel reinforced fly ash geopolymer concrete elements, Constr. Build. Mater. 90 (2015) 91–98.
[11] H.Y. Zhang et al., Thermal behavior and mechanical properties of geopolymer mortar after exposure to elevated temperatures, Constr. Build. Mater. 109 (2016) 17–24.
[12] W.D.A. Rickard, A. van Riessen, Performance of solid and cellular structured fly ash geopolymers exposed to a simulated fire, Cem. Concr. Compos. 48 (2014) 75–82.
[13] L. Zuda et al., Alkali-activated aluminosilicate composite with heat-resistant lightweight aggregates exposed to high temperatures: mechanical and water transport properties, Cem. Concr. Compos. 32 (2) (2010) 157–163.
[14] F.U.A. Shaikh, V. Vimonsatit, Compressive strength of fly-ash-based geopolymer concrete at elevated temperatures, Fire Mater. 39 (2015) 174–188.
[15] S. Bernal, R. Mejia de Gutierrez, F. Ruiz, H. Quiñonez, J.L. Provis, High temperature perfomrnace of mortars and concretes based on alkali-activated slag/metakaolin blends, Materiales de Construcción 62 (308) (2013) 471–488.
[16] T. Bakharev, Thermal behaviour of geopolymers prepared using class F fly ash and elevated temperature curing, Cem. Concr. Res. 36 (2006) 1134–1147.
[17] A. Fernández-Jiménez, A. Palomo, J.Y. Pastor, A. Martín, New cementitious materials based on alkali-activated fly ash: performance at high temperatures, J. Am. Ceram. Soc. 91 (2008) 3308–3314.
[18] J. Davidovits, Geopolymer Chemistry and Applications, Geopolymer Institute, Saint-Quentin, FR, 2017.
[19] V.F.F. Barbosa, K.J.D. MacKenzie, Thermal behaviour of inorganic geopolymers and composites derived from sodium polysialate, Mater. Res. Bull. 38 (2003) 319–331.
[20] A. Martin, J.Y. Pastor, A. Palomo, A. Fernández Jiménez, Mechanical behaviour at high temperature of alkali-activated aluminosilicates (geopolymers), Constr. Build. Mater. 93 (2015) 1188–1196.
[21] W.G.V. Saavedra, R.M. de Gutiérrez, Performance of geopolymer concrete composed of fly ash after exposure to elevated temperatures, Constr. Build. Mater. 154 (2017) 229–235.
[22] P. Duan, C. Yan, W. Zhou, Compressive strength and microstructure of fly ash based geopolymer blended with silica fume under thermal cycle, Cem. Concr. Compos. 78 (2017) 108–119.
[23] D.L.Y. Kong, J.G. Sanjayan, Damage behavior of geopolymer composites exposed to elevated temperatures, Cem. Concr. Compos. 30 (2008) 986–991.
[24] H.Y. Zhang, V. Kodur, S.L. Qi, B. Wu, Characterizing the bond strength of geopolymers at ambient and elevated temperatures, Cem. Concr. Compos. 58 (2015) 40–49.
[25] N. Ranjbar, M. Mehrali, A. Behnia, U.J. Alengaram, M.Z. Jumaat, Compressive strength and microstructural analysis of fly ash/palm oil fuel ash based geopolymer mortar, Mater. Des. 59 (2014) 532–539.
[26] H.T. Türker, M. Balçikanli, İ.H. Durmuş, E. Özbay, M. Erdemir, Microstructural alteration of alkali activated slag mortars depend on exposed high temperature level, Constr. Build. Mater. 104 (2016) 169–180.
[27] P.H.R. Borges, N. Banthia, H.A. Alcamand, W.L. Vasconcelos, E.H.M. Nunes, Performance of blended metakaolin/blastfurnace slag alkali-activated mortars, Cem. Concr. Compos. 71 (2016) 42–52.
[28] P. Duxson, G.C. Lukey, J.S.J. Van Deventer, Physical evolution of Na-geopolymer derived from metakaolin up to 1000 °C, J. Mater. Sci. 42 (9) (2007) 3044–3054.
[29] C. Tippayasam, P. Balyore, P. Thavorniti, E. Kamseu, C. Leonelli, P. Chindaprasirt, D. Chaysuwan, Potassium alkali concentration and heat treatment affected metakaolin-based geopolymer, Constr. Build. Mater. 104 (2016) 293–297.
[30] T. Yang, H. Zhu, Z. Zhang, Influence of fly ash on the pore structure and shrinkage characteristics of metakaolin-based geopolymer pastes and mortars, Constr. Build. Mater. 153 (2017) 284–293.
[31] N. Belmokhtar, M. Ammari, J. Brigui, L. Ben Allal, Comparison of the microstructure and the compressive strength of two geopolymers derived from Metakaolin and an industrial sludge, Construct. Build. Mater. 146 (2017) 621–629.
[32] L. Chen, Z. Wang, Y. Wang, J. Feng, Preparation and properties of alkali activated metakaolin-based geopolymer, Materials 9 (9) (2016) 1–12.
[33] H.K. Tchakouté, C.H. Rüscher, S. Kong, E. Kamseu, C. Leonelli, Geopolymer binders from metakaolin using sodium waterglass from waste glass and rice husk ash as alternative activators: A comparative study, Constr. Build. Mater. 114 (2016) 276–289.
[34] M. Gougazeh, Geopolymers from Jordanian metakaolin: Influence of chemical and mineralogical compositions on the development of mechanical properties, Jordan J. Civil Eng. 7 (2) (2013) 236–257.
[35] H. Wang, H. Li, F. Yan, Synthesis and mechanical properties of metakaolinite-based geopolymer, Colloids Surf., A 268 (1–3) (2005) 1–6.
[36] U.K. Sevim, Colemanite ore waste concrete with low shrinkage and high split tensile strength, Mater. Struct. 44 (1) (2011) 187–193.
[37] O. Gencel, W. Brostow, C. Ozel, M. Filiz, An investigation on the concrete properties containing colemanite, Int. J. Phys. Sci. 5 (2010) 216–225.
[38] I. Kula, A. Olgun, Y. Erdogan, V. Sevinc, Effects of colemanite waste, cool bottom ash, and fly ash on the properties of cement, Cem. Concr. Res. 31 (3) (2001) 491–494.
[39] M. Özdemir, N.U. Öztürk, Utilization of clay wastes containing boron as cement additives, Cem. Concr. Res. 33 (10) (2003) 1659–1661.
[40] Y.J. Ji, J.H. Cahyadi, Effects of densified silica fume on microstructure and compressive strength of blended cement pastes, Cem. Concr. Res. 33 (10) (2003) 1543–1548.
[41] H. Temiz, A.Y. Karakeci, An investigation on microstructure of cement paste containing fly ash and silica fume, Cem. Concr. Res. 32 (7) (2002) 1131–1132.
[42] Z.D. Rong, W. Sun, H.J. Xiao, W. Wang, Effect of silica fume and fly ash on hydration and microstructure evolution of cement based composites at low water-binder ratios, Constr. Build. Mater. 51 (2014) 446–450.
[43] M. Nili, A. Ehsani, Investigating the effect of the cement paste and transition zone on strength development of concrete containing nanosilica and silica fume, Mater. Des. 75 (2015) 174–183.
[44] D.O. Koteng, C.T. Chen, Strength development of lime-pozzolana pastes with silica fume and fly ash, Constr. Build. Mater. 84 (2015) 294–300.
[45] W. Wongkeo, P. Thongsanitgarn, A. Ngamjarurojana, A. Chaipanich, Compressive strength and chloride resistance of self-compacting concrete containing high level fly ash and silica fume, Mater. Des. 64 (2014) 261–269.
[46] A. Farahani, H. Taghaddos, M. Shekarchi, Prediction of long-term chloride diffusion in silica fume concrete in a marine environment, Cem. Concr. Comp. 59 (2015) 10–17.
[47] V. Lilkov, I. Rostovsky, O. Petrov, Y. Tzvetanova, P. Savov, Long term study of hardened cement pastes containing silica fume and fly ash, Constr. Build. Mater. 60 (2014) 48–56.
[48] P. Chindaprasirt, P. Paisitsrisawat, U. Rattanasak, Strength and resistance to sulfate and sulfuric acid of gound fluidized bed combustion fly ash-silica füme alkali-activated composite, Adv. Powder Technol. 25 (3) (2014) 1087–1093.
[49] M. Rostami, K. Behfarnia, The effect of silica fume on durability of alkali activated slag concrete, Constr. Build. Mater. 134 (2017) 262–268.
[50] N. Ranjbar, M. Mehrali, M. Mehrali, U.J. Alengaram, M.Z. Jumaat, Graphene nanoplatelet-fly ash based geopolymer composites, Cem. Concr. Res. 76 (2015) 222–231.
[51] D.R. Sahoo, A. Solanki, A. Kumar, Influence of steel and polypropylene fibers on flexural behavior of RC beams, J. Mater. Civ. Eng. 27 (8) (2014).
[52] N. Banthia, R. Gupta, Influence of polypropylene fiber geometry on plastic shrinkage cracking in concrete, Cem. Concr. Res. 36 (7) (2006) 1263–1267.

[53] W. Yao, J. Li, K. Wu, Mechanical properties of hybrid fiber-reinforced concrete at low fiber volume fraction, Cem. Concr. Res. 33 (1) (2003) 27–30.
[54] K.-H. Tan, P. Paramasivam, K.-C. Tan, Cracking characteristics of reinforced steel fiber concrete beams under short- and long-term loadings, Adv. Cem. Based Mater. 2 (4) (1995) 127–137.
[55] B.M. Tyson, R.K. Abu Al-Rub, A. Yazdanbakhsh, Z. Grasley, Carbon nanotubes and carbon nanofibers for enhancing the mechanical properties of nanocomposite cementitious materials, J. Mater. Civ. Eng. 23 (7) (2011) 1028–1035.
[56] P. Sukontasukkul, P. Pongsopha, P. Chindaprasirt, S. Songpiriyakij, Flexural performance and toughness of hybrid steel and polypropylene fibre reinforced geopolymer, Constr. Build. Mater. 161 (2018) 37–44.
[57] A. Bhutta, P.H.R. Borges, C. Zanotti, M. Farooq, N. Banthia, Flexural behavior of geopolymer composites reinforced with steel and polypropylene macro fibers, Cem. Concr. Compos. 80 (2017) 31–40.
[58] E. Mohseni, Assessment of Na_2SiO_3 to NaOH ratio impact on the performance of polypropylene fiber-reinforced geopolymer composites, Constr. Build. Mater. 186 (2018) 904–911.
[59] L. Du, K.J. Folliard, Mechanisms of air entrainment in concrete, Cem. Concr. Res. 35 (8) (2005) 1463–1471.
[60] Joseph F. Lamond, James H. Pielert, Significance of Tests and Properties of Concrete and Concrete-Making Materials, ASTM, West Conshohocken, PA, 2006.
[61] M. Pigeon, R. Pleau, Durability of Concrete in Cold Climates, CRC Press, 2010.
[62] H. Kim, J. Jeon, H. Lee, Workability, and mechanical, acoustic and thermal properties of lightweight aggregate concrete with a high volume of entrained air, Constr. Build. Mater. 29 (2012) 193–200.
[63] O. Sengul, S. Azizi, F. Karaosmanoglu, M.A. Tasdemir, Effect of expanded perlite on the mechanical properties and thermal conductivity of lightweight concrete, Energy Build. 43 (2) (2011) 671–676.
[64] B. Łaźniewska-Piekarczyk, The influence of selected new generation admixtures on the workability, air-voids parameters and frost-resistance of SCC, Constr. Build Mater. 31 (2012) 310–319.
[65] I. Vegas, J. Urreta, M. Frías, R. García, Freeze–thaw resistance of blended cements containing calcined paper sludge, Constr. Build. Mater. 23 (8) (2009) 2862–2868.
[66] C.-W. Chung, C.-S. Shon, Y.-S. Kim, Chloride ion diffusivity of fly ash and silica fume concretes exposed to freeze–thaw cycles, Constr. Build. Mater. 24 (9) (2010) 1739–1745.
[67] Y. Fu, L. Cai, Y. Wu, Freeze–thaw cycle test and damage mechanics models of alkali-activated slag concrete, Constr. Build. Mater. 25 (7) (2011) 3144–3148.
[68] S.A. Bernal, R.M. de Gutiérrez, J.L. Provis, Engineering and durability properties of concretes based on alkali-activated granulated blast furnace slag/metakaolin blends, Constr. Build. Mater. 33 (2012) 99–108.
[69] P. Sun, H.-C. Wu, Chemical and freeze–thaw resistance of fly ash-based inorganic mortars, Fuel 111 (2013) 740–745.
[70] L. Cai, H. Wang, Y. Fu, Freeze-thaw resistance of alkali-slag concrete based on response surface methodology, Constr. Build. Mater. 49 (2013) 70–76.
[71] Z. Yunsheng, S. Wei, L. Zongjin, Z. Xiangming, Eddie, C. Chungkong, Impact properties of geopolymer based extrudates incorporated with fly ash and PVA short fiber, Construct. Build. Mater. 22 (3) (2008) 370–383.
[72] A. Kampala, S. Horpibulsuk, N. Prongmanee, A. Chinkulkijniwat, Influence of wet-dry cycles on compressive strength of calcium carbide residue – fly ash stabilized clay, J. Mater. Civ. Eng. 26 (2014) 633–643.
[73] M. Lahoti, P. Narang, K.H. Tan, E. Yang, Mix design factors and strength prediction of metakaolin-based geopolymer, Ceram. Int. 43 (2017) 11433–11441.
[74] O. Burciaga-díaz, L.Y. Gómez-zamorano, J.I. Escalante-garcía, Influence of the long term curing temperature on the hydration of alkaline binders of blast furnace slag-metakaolin, Constr. Build. Mater. 113 (2016) 917–926.
[75] G. Görhan, R. Aslaner, O. Şinik, The effect of curing on the properties of metakaolin and fly ash-based geopolymer paste, Compos. B 97 (2016) 329–335.
[76] L. Yun-ming, H. Cheng-yong, L. Li, N. Ain, M. Mustafa, A. Al-Bakri, K. Hussin, Formation of one-part-mixing geopolymers and geopolymer ceramics from geopolymer powder, Constr. Build. Mater. 156 (2017) 9–18.
[77] K. Kaya, S. Soyer-uzun, Evolution of structural characteristics and compressive strength in red mud – metakaolin based geopolymer systems, Ceram. Int. 42 (2016) 7406–7413.
[78] A. Sabbatini, L. Vidal, C. Pettinari, I. Sobrados, S. Rossignol, Control of shaping and thermal resistance of metakaolin-based geopolymers, Mater. Des. 116 (2017) 374–385.
[79] O.G. Rivera, W.R. Long, C.A.W. Jr, R.D. Moser, B.A. Williams, K. Torres-cancel, P. G. Allison, Cement and Concrete Research Effect of elevated temperature on alkali-activated geopolymeric binders compared to portland cement-based binders, Cem. Concr. Res. 90 (2016) 43–51.
[80] Y. Aygörmez, O. Canpolat, M. Uysal, M.M. Al-mashhadani, Compressive and flexural strength behaviors of metakaolin based geopolymer mortars manufactured by different procedures, in: 4th International Conference on Green Design and Manufacture IConGDM 2030, 2018.
[81] M. Uysal, M.M. Al-mashhadani, Y. Aygörmez, O. Canpolat, Effect of using colemanite waste and silica fume as partial replacement on the performance of metakaolin-based geopolymer mortars, Constr. Build. Mater. 176 (2018) 271–282.
[82] A. Celik, K. Yilmaz, O. Canpolat, M.M. Al-mashhadani, Y. Aygörmez, M. Uysal, High-temperature behavior and mechanical characteristics of boron waste additive metakaolin based geopolymer composites reinforced with synthetic fibers, Constr. Build. Mater. 187 (2018) 1190–1203.
[83] A. Olgun, T. Kavas, Y. Erdogan, G. Once, Physico-chemical characteristics of chemically activated cement containing boron, Build. Environ. 42 (2007) 2384–2395.
[84] Y. Erdogan, M.S. Zeybek, A. Demirbas, Cement mixes containing colemanite from concentrator wastes, Cem. Concr. Res. 28 (4) (1998) 605–609.
[85] G.A. Rao, Investigations on the performance of silica fume-incorporated cement pastes and mortars, Cem. Concr. Res. 33 (2003) 1765–1770.
[86] ASTM C109 / C109M-16a, Standard Test Method for Compressive Strength of Hydraulic Cement Mortars (Using 2-in. or [50-mm] Cube Specimens), ASTM International, West Conshohocken, PA, 2016.
[87] ASTM C348-14, Standard Test Method for Flexural Strength of Hydraulic-Cement Mortars, ASTM International, West Conshohocken, PA, 2014.
[88] Y.J. Zhang, S. Li, Y.C. Wang, D.L. Xu, Microstructural and strength evolutions of geopolymer composite reinforced by resin exposed to elevated temperature, J. Non-Cryst. Solids 358 (3) (2012) 620–624.
[89] H.Y. Zhang, V. Kodur, P.E., F. ASCE, B. Wu, L. Cao, Qi S. Liang, Comparative thermal and mechanical performance of geopolymers derived from metakaolin and fly ash, J. Mater. Civ. Eng. 28 (2) (2016) 1–12.
[90] F. Uddin, Sh. Ahmed, Review of mechanical properties of short fibre reinforced geopolymer composites, Constr. Build. Mater. 43 (2013) 37–49.
[91] Zu.-hua Zhang, X. Yao, Hua-jun Zhu, et al., Preparation and mechanical properties of polypropylene fiber reinforced calcined kaolin-fly ash based geopolymer, J. Central South Univ. Technol. 16 (2009) 49–52.
[92] A. Natali, S. Manzi, M.C. Bignozzi, Novel fiber-reinforced composite materials based on sustainable geopolymer matrix, Proc. Eng. 20 (2011) 1124–1131.
[93] F. Xu, X. Deng, C. Peng, et al., Mix design and flexural toughness of PVA fiber reinforced fly ash-geopolymer composites, Construct. Build. Mater. 150 (2017) 179–189.
[94] M.Z. NazirKhan, Y. Hao, H. Hao, et al., Mechanical properties of ambient cured high strength hybrid steel and synthetic fibers reinforced geopolymer composites, Cem. Concr. Compos. 85 (2018) 133–152.
[95] M.M. Al-mashhadani, O. Canpolat, Y. Aygörmez, et al., Mechanical and microstructural characterization of fiber reinforced fly ash based geopolymer composites, Constr. Build. Mater. 167 (2018) 505–513.
[96] M. Viktor, A.S. Flávio, et al., Coupled strain rate and temperature effects on the tensile behavior of strain-hardening cement-based composites (SHCC) with PVA fibers, Cem. Concr. Res. 42 (2012) 1417–1427.
[97] R. Wang, C. Meyer, Performance of cement mortar made with recycled high impact polystyrene, Cem. Constr. Compos. 34 (2012) 975–981.
[98] G. Roviello, L. Ricciotti, O. Tarallo, et al., Innovative fly ash geopolymer-epoxy composites: preparation microstructure and mechanical properties, Materials 9 (2016) 461–476.
[99] P. Chindaprasirt, T. Chareerat, V. Sirivivatnanon, Workability and strength of coarse high calcium fly ash geopolymer, Cem. Concr. Compos. 29 (3) (2007) 224–229.
[100] A.M. López-buendía, M.D. Romero-sánchez, V. Climent, C. Guillem, Surface treated polypropylene (PP) fibres for reinforced concrete, Cem. Concr. Res. 54 (2013) 29–35.
[101] N. Ranjbar, M. Mehrali, A. Behnia, A. Javadi Pordsari, M. Mehrali, U.J. Alengaram, M.Z. Jumaat, A comprehensive study of the polypropylene fiber reinforced fly ash based geopolymer, PLoS One 11 (1) (2016) 1–20.
[102] I.B. Topçu, O.E. Demirel, T. Uygunoğlu, Physical and mechanical properties of polypropylene fiber reinforced mortars, J. Polytechn. 20 (1) (2017) 91–96.
[103] P. Pliya, A.L. Beaucour, A. Noumowé, Contribution of cocktail of polypropylene and steel fibres in improving the behavior of high strength concrete subjected to high temperature, Constr. Build. Mater. 25 (4) (2011) 1926–1934.
[104] Y. Ding, C. Azevedo, J.B. Aguiar, S. Jalali, Study on residual behaviour and flexural toughness of fibre cocktail reinforced self compacting high performance concrete after exposure to high temperature, Constr. Build. Mater. 26 (1) (2012) 21–31.
[105] N. Yermak, P. Pliya, A.-L. Beaucour, A. Simon, A. Noumowé, Influence of steel and/or polypropylene fibres on the behaviour of concrete at high temperature: spalling, transfer and mechanical properties, Constr. Build. Mater. 132 (2017) 240–250.
[106] E. Rudnik, T. Drzymała, Thermal behavior of polypropylene fiber-reinforced concrete at elevated temperatures, J. Therm. Anal. Calorim. 131 (2) (2018) 1005–1015.
[107] H.K. Shehab, A.S. Eisa, A.M. Wahba, Mechanical properties of fly ash based geopolymer concrete with full and partial cement replacement, Constr. Build. Mater. 126 (2016) 560–565.
[108] P. Kalifa, G. Chene, C. Galle, High-temperature behaviour of HPC with polypropylene fibers: from spalling to microstructure, Cem. Concr. Res. 31 (2001) 1487–1499.
[109] A.M. Rashad, S.R. Zeedan, A preliminary study of blended pastes of cement and quartz powder under the effect of elevated temperature, Constr. Build. Mater. 29 (2012) 672–681.
[110] S. Rafat, Utilization of silica fume in concrete: review of hardened properties, Resour. Conserv. Recycl. 55 (11) (2011) 923–932.
[111] A.C.A. Muller, K.L. Scrivener, J. Skibsted, A.M. Gajewicz, P.J. McDonald, Influence of silica fume on the microstructure of cement pastes: new insights from 1H NMR relaxometry, Cem. Concr. Res. 74 (2015) 116–125.
[112] A.J. Al-Tayyib, M.H. Baluch, M. Sharif Al-Farabi, M.M. Mahamud, The effect of thermal cycling on the durability of concrete made from local materials in the Arabian Gulf countries, Cem. Concr. Res. 19 (1989) 131–142.

[113] N.M. Akhras, K.M. Al-Akhras, M.F. Attom, Thermal cycling of wheat straw ash concrete, Constr. Mater. 161 (2008) 9–15.
[114] M. Maslehuddin, M. Sharif alfarabi, M. Shameem, M. Ibrahim, M.S. Barry, Comparison of properties of steel slag and crushed limestone aggregate concretes, Constr. Build. Mater. 17 (2003) 105–112.
[115] Cenk Karakurt, Properties of reinforced concrete steel rebars exposed to high temperatures, Adv. Mater. Sci. Eng. (2008).
[116] J. Eidan, I. Rasoolan, A. Rezaeian, D. Poorveis, Residual mechanical properties of polypropylene fiber-reinforced concrete after heating, Constr. Build. Mater. 198 (2019) 195–206.
[117] T.W. Cheng, M.L. Lee, M.S. Ko, T.H. Ueng, S.F. Yang, The heavy metal adsorption characteristics on metakaolin-based geopolymer, Appl. Clay Sci. 56 (2012) 90–96.
[118] D.L.Y. Kong, J.G. Sanjayan, K.S. Crentsil, Comparative performance of geopolymers made with metakaolin and fly ash after exposure to elevated temperatures, Cem. Concr. Res. 37 (2007) 1583–1589.
[119] K. Wang, Y. He, X. Song, X. Cui, Effects of the metakaolin-based geopolymer on high-temperature performances of geopolymer/PVC composite materials, Appl. Clay Sci. 114 (2015) 586–592.
[120] P. He, D. Jia, T. Lin, M. Wang, Y. Zhou, Effects of high-temperature heat treatment on the mechanical properties of unidirectional carbon fiber reinforced geopolymer composites, Ceram. Int. 36 (2010) 1447–1453.
[121] M. Lahoti, K.K. Wong, E. Yang, K.H. Tan, Effects of Si/Al molar ratio on strength endurance and volume stability of metakaolin geopolymers subject to elevated temperature, Ceram. Int. 44 (2018) 5726–5734.
[122] P.N. Hiremath, S.C. Yaragal, Performance evaluation of reactive powder concrete with polypropylene fibers at elevated temperatures, Constr. Build. Mater. 169 (2018) 499–512.
[123] P. Behera, V. Baheti, J. Militky, P. Louda, Elevated temperature properties of basalt microfibril filled geopolymer composites, Constr. Build. Mater. 163 (2018) 850–860.
[124] P. De Silva, K. Sagoe-Crenstil, Medium-term phase stability of Na_2O-Al_2O_3-SiO_2-H_2O geopolymer systems, Cem. Concr. Res. 38 (2008) 870–876.
[125] L.Y. Gomez-Zamorano, E. Vega-Cordero, L. Struble, Composite geopolymers of metakaolin and geothermal nanosilica waste, Constr. Build. Mater. 115 (2016) 269–276.
[126] A.M. Rashad, An exploratory study on sodium sulphate-activated slag blended with Portland cement under the effect of thermal loads, J. Therm. Anal. Calorim. 119 (2015) 1535–1545.
[127] X. Guo, H. Shi, W.A. Dick, Compressive strength and microstructural characteristics of class C fly ash geopolymer, Cem. Concr. Compos. 32 (2010) 142–147.
[128] J. Ye, W. Zhang, D. Shi, Effect of elevated temperature on the properties of geopolymer synthesized from calcined ore-dressing tailing of bauxite and ground-granulated blast furnace slag, Constr. Build. Mater. 69 (2014) 41–48.
[129] J. Temuujin, W. Ricard, M. Lee, A. Van Riessen, Preparation and thermal properties of fire resistant metakaolin-based Geopolymer-type coating, J. Non-Cryst. Solids 357 (2011) 1399–1404.
[130] O. Burciaga-Díaz, J.I. Escalante-Garcia, R.X. Magallanes-Rivera, Compressive strength and microstructural evolution of metakaolin geopolymers exposed to high temperature, ALCONPAT J. 5 (1) (2015) 52–66.
[131] S. Onutai, S. Jiemsirilers, P. Thavorniti, T. Kobayashi, Aluminium hydroxide waste based geopolymer composed of fly ash for sustainable cement materials, Constr. Build. Mater. 101 (2015) 298–308.
[132] Y.-L. Li, X.-L. Zhao, R.K.S. Raman, S. Al-Saadi, Thermal and mechanical properties of alkali-activated slag paste, mortar and concrete utilising seawater and sea sand, Constr. Build. Mater. 159 (2018) 704–724.
[133] A. Kashani, T.D. Ngo, B. Walkley, P. Mendis, Thermal performance of calcium-rich alkali-activated materials: A microstructural and mechanical study, Constr. Build. Mater. 153 (2017) 225–237.
[134] I.B. Topcu, O. Atesin, T. Uygunoglu, Effect of high dosage air-entraining admixture usage on micro concrete properties, Eur. J. Eng. Nat. Sci. (EJENS) 2 (1) (2017) 1–11.
[135] F. Puertas, T. Amat, A. Fernández-Jiménez, T. Vázquez, Mechanical and durable behaviour of alkaline cement mortars reinforced with polypropylene fibres, Cem. Concr. Res. 33 (12) (2003) 2031–2036.
[136] ASTM C348-14, Standard Test Method for Flexural Strength of Hydraulic-Cement Mortars, ASTM International, West Conshohocken, PA, 2014.
[137] M. Pigeon, R. Gagné, P.-C. Aitcin, N. Banthia, Freezing and thawing tests of high-strength concretes, Cem. Concr. Res. 21 (1991) 844–852.
[138] S. Pilehvar, A.M. Szczotok, J.F. Rodríguez, L. Valentini, M. Lanzón, R. Pamies, A.L. Kjøniksen, Effect of freeze-thaw cycles on the mechanical behavior of geopolymer concrete and Portland cement concrete containing micro-encapsulated phase change materials, Constr. Build. Mater. 200 (2019) 94–103.
[139] A. Allahverdi, M.M.B.R. Abadi, K.M. Anwar Hossain, M. Lachemi, Resistance of chemically-activated high phosphorous slag content cement against freeze–thaw cycles, Cold Regions Sci. Technol. 103 (Suppl. C) (2014) 107–114.
[140] L. Basheer, J. Kropp, D.J. Cleland, Assessment of the durability of concrete from its permeation properties: a review, Constr. Build. Mater. 15 (2) (2001) 93–103.
[141] P. Sun, H.C. Wu, Chemical and freeze-thaw resistance of fly ash-based inorganic mortars, Fuel 111 (2013) 740–745.
[142] Huai-Shuai Shang, Ting-Hua Yi, Freeze-thaw durability of air-entrained concrete, Sci. World J. (2013).
[143] F. Shahrajabian, K. Behfarnia, The effects of nano particles on freeze and thaw resistance of alkali-activated slag concrete, Constr. Build. Mater. 176 (2018) 172–178.
[144] A.A. Arslan, M. Uysal, A. Yılmaz, M.M. Al-mashhadani, O. Canpolat, F. Sahin, Y. Aygörmez, Influence of wetting-drying curing system on the performance of fiber reinforced metakaolin-based geopolymer composites, Constr. Build. Mater. 225 (2019) 909–926.
[145] R. Zhao, Y. Yuan, Z. Cheng, T. Wen, J. Li, F. Li, Z.J. Ma, Freeze-thaw resistance of Class F fly ash-based geopolymer concrete, Constr. Build. Mater. 222 (2019) 474–483.
[146] M. Zhao, G. Zhang, K.W. Htet, M. Kwon, C. Liu, Y. Xu, M. Tao, Freeze-thaw durability of red mud slurry-class F fly ash-based geopolymer: Effect of curing conditions, Constr. Build. Mater. 215 (2019) 381–390.
[147] M.W. Hussin, A. Nur Farhayu, M.A.R. Bhutta, A.S.L. Nor Hasanah, Study on dry-wet cyclic resistance of geopolymer mortars using blended ash from agro-industrial waste, in: Third International Conference on Sustainable Construction Materials and Technologies (2013).
[148] J.C. Petermann, A. Saeed, M.I. Hammons, Alkali-activated Geopolymers: A Literature Review Air Force Research Laboratory Materials and Manufacturing Directorate, 2010.
[149] M. Hoy, R. Rachan, S. Horpibulsuk, A. Arulrajah, M. Mirzababaei, Effect of wetting–drying cycles on compressive strength and microstructure of recycled asphalt pavement – Fly ash geopolymer, Constr. Build. Mater. 144 (2017) 624–634.